PHYSICAL REVIEW D **67**, 083516 (2003)

Correlation-consistency cartography of the double-inflation landscape

Shinji Tsujikawa
Research Center for the Early Universe, University of Tokyo, Hongo, Bunkyo-ku, Tokyo 113-0033, Japan

David Parkinson and Bruce A. Bassett
Institute of Cosmology and Gravitation, University of Portsmouth, Mercantile House, Portsmouth PO1 2EG, United Kingdom

(Received 15 October 2002; published 29 April 2003)

We show explicitly some exciting features of double inflation: (i) it can often lead to strongly correlated adiabatic and entropy (isocurvature) power spectra; (ii) the two-field slow-roll consistency relations can be violated when the correlation is large at the Hubble crossing; (iii) the spectra of adiabatic and entropy perturbations can be strongly scale dependent and tilted toward either the red or blue. These effects are typically due to a light or time-dependent entropy mass and a non-negligible angular velocity in field space during inflation. They are illustrated via a multiparameter numerical search for correlations in two concrete models. The correlation is found to be particularly strong in a supersymmetric scenario due to the rapid growth of entropy perturbations in the tachyonic region separating the two inflationary stages. Our analysis suggests that realistic double-inflation models will provide a rich and fruitful arena for the application of future cosmic data sets and new approximation schemes which go beyond slow roll.

DOI: 10.1103/PhysRevD.67.083516 PACS number(s): 98.80.Cq

I. INTRODUCTION

One of the radical developments in recent inflationary research has been the realization—implicit in early work [1]—that inflationary predictions for the cosmic microwave background (CMB) and large-scale structure (LSS) can depend sensitively on postinflationary, but pre-photon-decoupling, physics. This is a departure from the single-field inflationary paradigm [2] that has been the backbone of high-energy cosmology over the past 20 years. This rather subtle paradigm shift can be primarily attributed to the driving force of particle physics inflationary models [3] which necessarily involve more than one dynamically important field and often lead to more than one phase of inflation [4].

The key point about multifield models of inflation for this paper is that they allow for substantial super-Hubble entropy or isocurvature perturbations [5] (see also Refs. [6], [7]). This implies a very interesting dynamics since, *at linear order*, entropy perturbations source adiabatic perturbations while the converse is not true in the large-scale limit [8] (although see the counterclaims in [9]). Further, these entropy modes can be partially or completely correlated with the adiabatic modes, and this correlation[1] is both important for the CMB and sensitive to the way in which reheating occurs.

Our aim in this paper is to provide the first exhaustive study of adiabatic-entropy correlations in ''realistic'' double-inflation models. Given that the current CMB data actually favor such a correlated mixture [10], there exists the exciting possibility that upcoming data will allow us to significantly constrain realistic inflationary parameter spaces.

Let us briefly recap the areas discovered so far for which entropy perturbations can be important.

Perturbations in multifield inflationary models [11–34]—models with two or more phases of inflation typically lead to some correlation due to the curvature of the phase curves in field space. This correlation can be preserved or wiped out depending on the precise details of reheating.

The curvaton [35]—an entropy perturbation can be converted into an adiabatic perturbation with a total correlation.

Preheating [36]—the nonperturbative, resonant decay of the inflaton can affect standard inflationary predictions for the CMB in certain special cases where there is an entropy perturbation on large scales that is resonantly amplified at preheating.

The possibility of correlated mixtures of adiabatic and isocurvature perturbations is both exciting and depressing for phenomenology. Instead of a single (adiabatic) power spectrum, one needs a matrix of power spectra [37,38] describing the full correlation network for the complex cosmic mixture of fluids. In addition the evolution of the correlation power spectra is very sensitive to the way in which particle decays occur after inflation. The precise nature of decay channels and widths during and after reheating can preserve or wash out preexisting correlations, introducing new arbitrary parameters but also opening up a new window on particle physics beyond the inflaton potential. Multifield models may also lead to significant levels of non-Gaussianity in the CMB transferred from the entropy to adiabatic modes [39].

There are still unresolved issues in the multifield context. In particular, the validity of the slow-roll approximation has not been fully explored. Indeed, this is one of the aims of our analysis. In addition, new effects occur in the case when the kinetic terms of the scalar fields are not canonical (e.g., the nonlinear sigma model) and hence parametrize a curved manifold, as occurs in the case of scalar-tensor theories [15,16,32] and string-inspired cosmologies [40].

An analysis of scalar perturbations in such a general situation has been studied [16,20] but only under the assumption of the slow roll. Even in the single-field case the slow-roll

[1]This mode-mode correlation is to be contrasted with the time-dependent correlations of [12].

approximation can introduce errors in the calculation of the CMB spectrum of up to 15% [41] and going to higher order in the slow-roll parameters may be necessary [42]. The situation in the more general case is clearly more subtle.

Recently Bartolo *et al.* [31] investigated the spectra of correlated perturbations and the modification of the standard consistency relation $n_T=-2r_T$ using the slow-roll analysis in the multifield context. (Here n_T is the spectral index of the gravitational wave and r_T is the relative amplitude of tensor to scalar perturbations.) According to their results, the single-field consistency relation is significantly modified when the correlation r_C between adiabatic and isocurvature perturbations is strong, as follows.

The first consistency relation:

$$r_T=-\frac{n_T}{2}(1-r_C^2). \tag{1.1}$$

In addition to the standard slow-roll approximation where the second-order derivatives of scalar fields are neglected, Bartolo *et al.* assumed that the adiabatic/entropy mass and the scalar field velocity angle evolve slowly during the multiple phases of inflation. While the latter approximation is generally valid in the single-field context, this is not so in models with two stages of inflation because the masses of field perturbations as well as the slow-roll parameters already get large around the end of the *first* stage of inflation. Making use of this approximation, Bartolo *et al.* derived a second consistency relation [31].

The second consistency relation:

$$(n_C-n_S)r_T=-\frac{n_T}{4}(2n_C-n_{\mathcal{R}}-n_S), \tag{1.2}$$

where $n_{\mathcal{R}}$, n_S, and n_C are the spectral indices of curvature perturbations, isocurvature perturbations, and their correlations, respectively.

More recently, Wands *et al.* [34] rederived the first of the consistency relations (the multifield version of the standard single-field consistency relation), assuming slow roll only *at* horizon crossing. On the other hand the slow-roll approximation during the whole stage of inflation is required to obtain the second consistency relation (we will explain this issue in the next section).

In this work we shall consider the more general situation where the slow-roll conditions are not necessarily satisfied even at horizon crossing and check the validity of the two consistency relations numerically in ''realistic'' double-inflation models. The models we adopt are the double inflation with two massive scalar fields (both noninteracting [13,14,24] and interacting [18]) and the two-stage supersymmetric inflation with tachyonic (spinodal) instability [43–45] where the second derivative of the potential becomes negative.

The former model is probably the simplest double-inflation generalization of the chaotic inflationary scenario. The second model is motivated by supersymmetric theories [46–51], in which case the potentials of scalar fields generically have tachyonic instability regions. Since these two kinds of model include the basic properties of double inflation, it is straightforward to extend our analysis to other double-inflationary scenarios.

We organize our paper as follows. In Sec. II we present the general framework of our analysis including the multi-field decomposition into adiabatic and entropy field perturbations and the resulting power spectra of correlated density perturbations. We also discuss the limitation of the slow-roll approximation in the multifield context. In Sec. III we analyze the model with two massive scalar fields. Section IV is devoted to the double inflation with a tachyonic instability while the final section concludes.

II. GENERAL FRAMEWORK

Let us consider two-field inflation with minimally coupled scalar fields ϕ and χ with a potential $V(\phi,\chi)$. In a flat Friedmann-Lemaitre-Robertson-Walker (FLRW) background with a scale factor a, the background equations are

$$H^2\equiv\left(\frac{\dot a}{a}\right)^2=\frac{\kappa^2}{3}\left(\frac{1}{2}\dot\phi^2+\frac{1}{2}\dot\chi^2+V\right),\quad \dot H=-\frac{\kappa^2}{2}(\dot\phi^2+\dot\chi^2), \tag{2.1}$$

$$\ddot\phi+3H\dot\phi+V_\phi=0,\quad \ddot\chi+3H\dot\chi+V_\chi=0, \tag{2.2}$$

where $V_\phi\equiv\partial V/\partial\phi$, H is the Hubble expansion rate, and $\kappa^2=8\pi/M_p^2$ with M_p being the Planck mass. At linear order minimally coupled scalar fields do not induce an anisotropic stress [6,7,52] and hence scalar metric perturbations can be characterized by a single potential Φ. The metric in the longitudinal gauge then becomes

$$ds^2=-(1+2\Phi)dt^2+a^2(1-2\Phi)\delta_{ij}dx^idx^j. \tag{2.3}$$

The Fourier transformed, linearized Einstein equations for field and metric perturbations in this gauge are

$$\dot\Phi+H\Phi=\frac{\kappa^2}{2}(\dot\phi\delta\phi+\dot\chi\delta\chi), \tag{2.4}$$

$$\delta\ddot\phi+3H\delta\dot\phi+\left(\frac{k^2}{a^2}+V_{\phi\phi}\right)\delta\phi=-2V_\phi\Phi+4\dot\phi\dot\Phi-V_{\phi\chi}\delta\chi, \tag{2.5}$$

$$\delta\ddot\chi+3H\delta\dot\chi+\left(\frac{k^2}{a^2}+V_{\chi\chi}\right)\delta\chi=-2V_\chi\Phi+4\dot\chi\dot\Phi-V_{\phi\chi}\delta\phi, \tag{2.6}$$

where k is the comoving momentum (wave number). All first order quantities in the equations that follow are functions of both k and t (the k subscript is implicit).[2]

We now provide a self-contained review of the decomposition of adiabatic and isocurvature scalar field perturbations [8] and the resulting spectra of correlated perturbations [31].

[2]In this paper we will often use the phrase ''horizon crossing.'' This should be read ''Hubble radius crossing'' occurring for a mode with wave number k when $k=aH$.

These two papers are our basic references in this section and we will, where possible, follow their notation.

We will then also discuss the limitations of results obtained using slow-roll analysis.

Let us first introduce the ''adiabatic'' field σ and the ''entropy'' field s defined by

$$d\sigma = (\cos\theta)d\phi + (\sin\theta)d\chi,$$
$$ds = -(\sin\theta)d\phi + (\cos\theta)d\chi. \tag{2.7}$$

Here θ is the angle of the trajectory in field space, satisfying $\tan\theta = \dot{\chi}/\dot{\phi}$. With an effective potential $V(\phi,\chi)$, the equations for adiabatic and entropy field perturbations are written in the form [8]

$$\delta\ddot{\sigma} + 3H\delta\dot{\sigma} + \left(\frac{k^2}{a^2} + V_{\sigma\sigma} - \dot{\theta}^2\right)\delta\sigma = -2V_\sigma\Phi + 4\dot{\sigma}\dot{\Phi} + 2(\dot{\theta}\delta s)^{\cdot} - \frac{2V_\sigma}{\dot{\sigma}}\dot{\theta}\delta s, \tag{2.8}$$

$$\delta\ddot{s} + 3H\delta\dot{s} + \left(\frac{k^2}{a^2} + V_{ss} + 3\dot{\theta}^2\right)\delta s = \frac{\dot{\theta}}{\dot{\sigma}}\frac{k^2}{2\pi G a^2}\Phi, \tag{2.9}$$

where

$$V_{\sigma\sigma} = (\cos^2\theta)V_{\phi\phi} + (\sin 2\theta)V_{\phi\chi} + (\sin^2\theta)V_{\chi\chi}, \tag{2.10}$$

$$V_{ss} = (\sin^2\theta)V_{\phi\phi} - (\sin 2\theta)V_{\phi\chi} + (\cos^2\theta)V_{\chi\chi}. \tag{2.11}$$

From Eq. (2.4) we have

$$\Phi = \frac{\kappa^2}{2a}\int a\dot{\sigma}\delta\sigma\, dt. \tag{2.12}$$

This indicates that the gravitational potential is sourced by the adiabatic field perturbation.

Introducing the Sasaki-Mukhanov variable [53]

$$Q_\sigma \equiv \delta\sigma + \frac{\dot{\sigma}}{H}\Phi, \tag{2.13}$$

the equation for the adiabatic field perturbation can be rewritten as [8]

$$\ddot{Q}_\sigma + 3H\dot{Q}_\sigma + \left[\frac{k^2}{a^2} + V_{\sigma\sigma} - \dot{\theta}^2 - \frac{\kappa^2}{a^3}\left(\frac{a^3\dot{\sigma}^2}{H}\right)^{\cdot}\right]Q_\sigma = 2(\dot{\theta}\delta s)^{\cdot} - 2\left(\frac{V_\sigma}{\dot{\sigma}} + \frac{\dot{H}}{H}\right)\dot{\theta}\delta s. \tag{2.14}$$

The slow-roll solutions for Q_σ and δs can be obtained by neglecting the second-order derivatives ($\ddot{Q}_\sigma$ and $\delta\ddot{s}$) in Eqs. (2.14) and (2.9). The evolution of fluctuations using this slow-roll approximation shows fairly good agreement with numerical results except around the end of inflation [32], unless there exists an intermediate noninflationary stage (see Ref. [13]). Other kinds of slow-roll approximations discussed later are more problematic, however.

Note, however, that neglecting the second-order derivatives in Eqs. (2.14) and (2.9) still leads to deviation of the power spectra at the *end* of inflation as found in numerical simulations in Ref. [32]. In this work, we numerically follow the evolution of perturbations during double inflation and estimate the spectra right after the end of inflation.

To provide the comparison to our full numerical results consider the solutions for Eqs. (2.14) and (2.9), found by neglecting $\ddot{Q}_\sigma$ and $\delta\ddot{s}$ [31]. These solutions correspond to neglecting the decaying modes of Q_σ and δs. Then one has

$$Q_\sigma \simeq Af(t) + BP(t), \quad \delta s \simeq Bg(t). \tag{2.15}$$

Here $A = A(k)$ and $B = B(k)$. When $f = g = 1$ and $P = 0$ at horizon crossing ($k = aH$), the amplitudes A and B are determined by the quantum fluctuations within the Hubble radius:

$$A = \frac{H_k}{\sqrt{2k^3}}e_Q(\mathbf{k}), \quad B = \frac{H_k}{\sqrt{2k^3}}e_s(\mathbf{k}). \tag{2.16}$$

Here $e_Q(\mathbf{k})$ and $e_s(\mathbf{k})$ are classical stochastic Gaussian quantities, satisfying $\langle e_Q(\mathbf{k})\rangle = \langle e_s(\mathbf{k})\rangle = 0$ and $\langle e_i(\mathbf{k})e_j^*(\mathbf{k}')\rangle = \delta_{ij}\delta^{(3)}(\mathbf{k}-\mathbf{k}')$. Note that H_k is the Hubble parameter at horizon crossing. We caution the reader that in the context of double inflation P can be nonzero at horizon crossing due to strong correlations. Clearly then the assumption of uncorrelated adiabatic and entropy perturbations at $k = aH$ is not generally justified. In order to make an accurate numerical analysis we choose the Bunch-Davies vacuum state deep inside the horizon ($k \gg aH$) so that the $\dot{\theta}$ term in the right-hand side (RHS) of Eq. (2.14) is negligible initially.

On super-Hubble scales ($k \ll aH$) the slow-roll solution for δs can be written as

$$g(t) = \exp\left(-\int_{N(t)}^{N_k}\frac{\mu_s^2}{3H^2}dN\right) \simeq \exp\left[-\frac{\mu_s^2}{3H^2}[N_k - N(t)]\right], \tag{2.17}$$

where $\mu_s^2 \equiv V_{ss} + 3\dot{\theta}^2$ and $N(t) = -\int_{t_f}^{t} H\, dt$ with t_f being the time at the end of inflation. The quantity $N_k = -\int_{t_f}^{t_k} H\, dt$ corresponds to the e-folding between the horizon crossing and the end of inflation.

In deriving Eq. (2.17) the time dependence of the $-\mu_s^2/(3H^2)$ term has been neglected, and this term is pulled out of the integral. In the single-field inflationary scenario, the variation of this term is associated with the end of inflation, in which case the error in this approximation is not significant for cosmologically relevant scales. In the case of double inflation, the situation is quite different. Since the mass term $-\mu_s^2/(3H^2)$ already grows large at the end of the *first* stage of inflation, the assumption that the value of $-\mu_s^2/(3H^2)$ will not change during *both* stages of inflation is not generally valid. In fact we shall numerically show later

that this term typically changes significantly during double inflation. This casts doubts on results derived using this approximation and suggests that a more sophisticated approximation may be needed to handle multiple phases of inflation completely.

The slow-roll expansion for $-\mu_s^2/(3H^2)$ is given by [31]

$$-\frac{\mu_s^2}{3H^2}=-\frac{\epsilon_\chi\eta_{\phi\phi}+\epsilon_\phi\eta_{\chi\chi}}{\epsilon_t}+2\frac{(\pm\sqrt{\epsilon_\phi})(\pm\sqrt{\epsilon_\chi})}{\epsilon_t}\eta_{\phi\chi}, \tag{2.18}$$

where the slow-roll parameters are defined by

$$\epsilon_I\equiv\frac{1}{2\kappa^2}\left(\frac{V_{\phi I}}{V}\right)^2, \quad \eta_{IJ}\equiv\frac{1}{\kappa^2}\frac{V_{\phi I\phi,I}}{V}, \tag{2.19}$$

with $\epsilon_t\equiv\epsilon_\phi+\epsilon_\chi$. The entropy field perturbation at the end of inflation is approximately expressed as Eq. (2.17) with

$$g(t_f)=\exp\left[\left(-\frac{\epsilon_\chi\eta_{\phi\phi}+\epsilon_\phi\eta_{\chi\chi}}{\epsilon_t}+2\frac{(\pm\sqrt{\epsilon_\phi})(\pm\sqrt{\epsilon_\chi})}{\epsilon_t}\eta_{\phi\chi}\right)_k N_k\right], \tag{2.20}$$

where we set $N(t_f)=0$. The slow-roll parameters in this expression are evaluated at horizon crossing $k=aH$, since the constancy of the mass term is assumed in Eq. (2.17) [the subscript k in Eq. (2.20) denotes the value at horizon crossing].

The slow-roll solution for Q_σ at the end of inflation can be obtained by assuming the constancy of $\mu_Q^2/H^2\equiv[V_{\sigma\sigma}-\dot\theta^2-\kappa^2a^{-3}(a^3\dot\sigma^2/H)^{\cdot}]/H^2$ and $\dot\theta/H$ as

$$f(t_f)=\exp\left[\left(-\frac{\epsilon_\chi\eta_{\chi\chi}+\epsilon_\phi\eta_{\phi\phi}}{\epsilon_t}-2\frac{(\pm\sqrt{\epsilon_\phi})(\pm\sqrt{\epsilon_\chi})}{\epsilon_t}\eta_{\phi\chi}+2\epsilon_t\right)_k N_k\right],$$

$$P(t_f)=2g(t_f)\left(\frac{\dot\theta}{H}\right)_k\frac{e^{\zeta_k N_k}-1}{\zeta_k}, \tag{2.21}$$

where

$$\zeta\equiv\frac{\mu_s^2-\mu_Q^2}{3H^2}=\frac{(\epsilon_\phi-\epsilon_\chi)(\eta_{\chi\chi}-\eta_{\phi\phi})}{\epsilon_t}-4\frac{(\pm\sqrt{\epsilon_\phi})(\pm\sqrt{\epsilon_\chi})}{\epsilon_t}\eta_{\phi\chi}+2\epsilon_t \tag{2.22}$$

and

$$\frac{\dot\theta}{H}=\frac{\epsilon_\phi-\epsilon_\chi}{\epsilon_t}\eta_{\phi\chi}+\frac{(\pm\sqrt{\epsilon_\phi})(\pm\sqrt{\epsilon_\chi})}{\epsilon_t}(\eta_{\phi\phi}-\eta_{\chi\chi}). \tag{2.23}$$

In Eq. (2.21) ζ_k and $(\dot\theta/H)_k$ are evaluated at horizon crossing due to the assumption of time independence during inflation. This assumption is not generally justified in the context of the double inflation, as we already mentioned.

The curvature perturbation $\mathcal{R}$ is defined by [8]

$$\mathcal{R}\equiv\Phi+H\frac{\dot\phi\,\delta\phi+\dot\chi\,\delta\chi}{\dot\phi^2+\dot\chi^2}=\frac{H}{\dot\sigma}Q_\sigma. \tag{2.24}$$

Since the time derivative of $\mathcal{R}$ is given by [53,8]

$$\dot{\mathcal{R}}=\frac{H}{\dot H}\frac{k^2}{a^2}\Phi+\frac{2H}{\dot\sigma}\dot\theta\delta s, \tag{2.25}$$

the curvature perturbation is not conserved even in the large-scale limit ($k\to0$) in the presence of the entropy field perturbation δs. Therefore the constancy of $\mathcal{R}$ that is typically assumed in the slow-roll single-field inflationary scenario is not valid in the multifield case. Instead, we need to estimate the power spectrum of $\mathcal{R}$ at the end of inflation from Eq. (2.15) as

$$\mathcal{P}_\mathcal{R}=\left(\frac{H_k}{2\pi}\right)^2\frac{H^2(t_f)}{\dot\sigma^2(t_f)}[|f^2(t_f)|+|P^2(t_f)|]\simeq\frac{1}{\pi}\left(\frac{H_k}{M_p}\right)^2\frac{1}{\epsilon_t(t_f)}[|f^2(t_f)|+|P^2(t_f)|]. \tag{2.26}$$

The isocurvature perturbation of two scalar fields χ and ϕ is defined by [6]

$$S_{\chi\phi}\equiv\frac{\delta\rho_\chi}{\rho_\chi+p_\chi}-\frac{\delta\rho_\phi}{\rho_\phi+p_\phi}=\dot\delta_{\chi\phi}-3H\delta_{\chi\phi}, \tag{2.27}$$

where $\delta_{\chi\phi}\equiv\delta_{\chi/\dot\chi}-\delta\phi/\dot\phi=\dot\sigma/(\dot\phi\dot\chi)\,\delta s$. Neglecting the contribution from the $\delta\dot s$ term, the isocurvature perturbation can be written in terms of the entropy field perturbation δs as

$$S_{\chi\phi}=T_{\chi\phi}\delta s \quad \text{with} \quad T_{\chi\phi}\simeq-3\frac{\sqrt{4\pi}}{M_p}\frac{\sqrt{\epsilon_t}}{(\pm\sqrt{\epsilon_\phi})(\pm\sqrt{\epsilon_\chi})}. \tag{2.28}$$

We note that when the slow-roll conditions are violated the $\delta\dot s$ term may provide a contribution to the isocurvature perturbation that is not captured by Eq. (2.28), which can induce small differences when compared with the definition (2.27).

Making use of Eq. (2.28), the power spectrum of the isocurvature perturbation at the end of inflation is found to be

$$\mathcal{P}_S=\left(\frac{H_k}{2\pi}\right)^2T_{\chi\phi}^2|g^2(t_f)|\simeq\frac{9}{\pi}\left(\frac{H_k}{M_p}\right)^2\frac{\epsilon_t(t_f)}{\epsilon_\phi(t_f)\epsilon_\chi(t_f)}|g^2(t_f)|. \tag{2.29}$$

The cross spectrum between Q_σ and δs is estimated as $P_{Q\delta s}=(H_k/2\pi)^2g(t)P(t)$ from Eq. (2.15). Then we find the cross spectrum between $\mathcal{R}$ and S as

$$\mathcal{P}_C=\left(\frac{H_k}{2\pi}\right)^2\frac{H(t_f)}{\dot\sigma(t_f)}T_{\chi\phi}g(t_f)P(t_f)$$
$$\simeq-\frac{6}{\pi}\left(\frac{\dot\theta}{H}\right)_k\left(\frac{H_k}{M_p}\right)^2$$
$$\times\frac{e^{\zeta_k N_k}-1}{\zeta_k}\frac{|g^2(t_f)|}{[\pm\sqrt{\epsilon_\phi(t_f)}][\pm\sqrt{\epsilon_\chi(t_f)}]}. \quad (2.30)$$

The spectral indices for the power spectrum $\mathcal{P}$ are defined by

$$n-1\equiv\frac{d\ln\mathcal{P}}{d\ln k}=(1+\epsilon_t)\left.\frac{d\ln\mathcal{P}}{d\ln a}\right|_{k=aH} \quad (2.31)$$

Therefore the spectral indices for $\mathcal{P}_\mathcal{R}$, $\mathcal{P}_S$, and $\mathcal{P}_C$ read [31]

$$n_\mathcal{R}-1=-6\epsilon_t+2\frac{\epsilon_\phi\eta_{\phi\phi}+\epsilon_\chi\eta_{\chi\chi}}{\epsilon_t}+4\frac{(\pm\sqrt{\epsilon_\phi})(\pm\sqrt{\epsilon_\chi})}{\epsilon_t}\eta_{\phi\chi}$$
$$-\frac{8|f^2(t_f)|}{|f^2(t_f)|+|P^2(t_f)|}\left(\frac{\dot\theta}{H}\right)_k^2\frac{e^{-\zeta_k N_k}}{\zeta_k}(1-e^{-\zeta_k N_k}), \quad (2.32)$$

$$n_S-1=-2\epsilon_t+2\frac{\epsilon_\phi\eta_{\chi\chi}+\epsilon_\chi\eta_{\phi\phi}}{\epsilon_t}$$
$$-4\frac{(\pm\sqrt{\epsilon_\phi})(\pm\sqrt{\epsilon_\chi})}{\epsilon_t}\eta_{\phi\chi}, \quad (2.33)$$

$$n_C-1=-2\epsilon_t+2\frac{\epsilon_\phi\eta_{\chi\chi}+\epsilon_\chi\eta_{\phi\phi}}{\epsilon_t}-4\frac{(\pm\sqrt{\epsilon_\phi})(\pm\sqrt{\epsilon_\chi})}{\epsilon_t}\eta_{\phi\chi}$$
$$-\frac{\zeta_k e^{\zeta_k N_k}}{e^{\zeta_k N_k}-1}, \quad (2.34)$$

where the slow-roll parameters are evaluated at horizon crossing. The spectrum P_T and the spectral index n_T of tensor perturbations are calculated by analyzing the equation of massless gravitational fields [3]:

$$P_T=\left(\frac{4}{\sqrt{\pi}}\frac{H_k}{M_p}\right)^2, \quad n_T=-\frac{8\pi}{M_p^2}\left(\frac{\dot\sigma}{H}\right)_k^2. \quad (2.35)$$

We introduce two ratios r_C and r_T, which are defined as

$$r_C\equiv\frac{P_C}{\sqrt{P_\mathcal{R}P_S}} \quad (2.36)$$

and

$$r_T\equiv\frac{P_T}{16P_\mathcal{R}}. \quad (2.37)$$

From Eqs. (2.26), (2.29), and (2.30) we find that the correlation ratio r_C can be expressed as

$$r_C=\frac{x}{\sqrt{1+x^2}} \quad \text{with} \quad x=\frac{P(t_f)}{f(t_f)}. \quad (2.38)$$

Therefore r_C^2 lies in the range $0\leqslant r_C^2\leqslant 1$. Note that the relation (2.38) is obtained without assuming that the adiabatic/entropy masses and $\dot\theta/H$ are constant after horizon crossing; namely, the equality $\simeq$ in Eqs. (2.26), (2.29), and (2.30) is not used when we derive Eq. (2.38). If the slow-roll solutions (2.21) are employed, we have

$$x\simeq 2\left(\frac{\dot\theta}{H}\right)_k\frac{1-e^{-\zeta_k N_k}}{\zeta_k}. \quad (2.39)$$

The behavior of the term $\dot\theta/H$ is most important when we analyze the correlation between adiabatic and isocurvature perturbations. In Eq. (2.39) the ''frozen'' value of $\dot\theta/H$ is used at horizon crossing. However, since the assumption of constant $\dot\theta/H$ is not generally valid during double inflation, the slow-roll result (2.39) leads to some errors in estimating r_C at the end of double inflation. When $\dot\theta/H$ varies significantly, we have to integrate this term from first horizon crossing to the end of inflation rather than use the ''frozen'' value at horizon crossing. Note that if $\dot\theta/H$ is vanishingly small during *both* phases of inflation the correlation vanishes ($r_C=0$).

The tensor to scalar ratio r_T can be evaluated without using the slow-roll equality in Eqs. (2.26) and (2.35) as

$$r_T=\frac{4\pi}{M_p^2}\left(\frac{\dot\sigma(t_f)}{H(t_f)}\right)^2\frac{1}{|f^2(t_f)|+|P^2(t_f)|}=\frac{4\pi}{M_p^2}\left(\frac{\dot\sigma}{H}\right)_k^2\frac{1}{1+x^2}. \quad (2.40)$$

Here we used the fact that $(H/\dot\sigma)f$ is conserved after horizon crossing, i.e., $(H/\dot\sigma)_k=[H(t_f)/\dot\sigma(t_f)]f(t_f)$ [see Eq. (2.25) with $k\ll aH$ and $\delta s=0$]. Making use of Eqs. (2.35), (2.38), and (2.40) we get the consistency relation

$$r_T=-\frac{n_T}{2}(1-r_C^2). \quad (2.41)$$

This indicates that the correlation between adiabatic and isocurvature perturbations leads to the modification of the consistency relation in the single-field case ($r_T=-n_T/2$).

In deriving Eq. (2.41), we did not exploit the assumption that the adiabatic/entropy mass and $\dot\theta/H$ are constant after horizon crossing. Then this consistency relation should be valid as long as the slow-roll conditions are satisfied *at horizon crossing*, in which case the uncorrelated solutions for Q_σ and δs can be used at $k=aH$ [34].[3] In the context of double inflation there are some cases where the slow-roll conditions can be violated at horizon crossing, implying that

[3]Note that the decaying mode for $\mathcal{R}$ can be important in some non-slow-roll inflationary scenarios [54,55]. In this case the second derivatives of Eqs. (2.9) and (2.14) are not necessarily small and the first term in the RHS of Eq. (2.15) is not negligible. Then we need to add the decaying mode solutions to Eq. (2.15). The consistency relation (2.41) does not cover this case, although the enhancement of the decaying mode occurs only in some restricted situations [54,55].

the consistency relation (2.41) does not hold automatically when applied to realistic double-inflation models.

The authors in Ref. [31] obtained the following second consistency relation from the slow-roll results (2.32), (2.34) together with Eqs. (2.35) and (2.40) as

$$(n_C - n_S) r_T = -\frac{n_T}{4}(2n_C - n_{\mathcal{R}} - n_S). \tag{2.42}$$

Note that the constancy of the adiabatic/entropy mass and $\dot{\theta}/H$ is assumed in deriving this relation. Therefore it is likely that the second consistency relation (2.42) is more strongly affected by the violation of the slow-roll conditions compared to the first consistency relation (2.41).

While the slow-roll results which include the quantities $n_{\mathcal{R}}$, n_S, and n_C can exhibit strong deviation from the numerical results, the spectral index n_T of the gravitational wave is well described by Eq. (2.35) even in the context of double inflation. Therefore, provided that the correlation is small at horizon crossing, the first consistency relation (2.41) is expected to be reliable as long as we use x in Eq. (2.38) instead of the slow-roll result in Eq. (2.39).

In the following section we shall compare the above formula with full numerical simulations for concrete models of double inflation (see the Appendix for the numerical method to evaluate power spectra and correlations). We will provide a detailed analysis of the spectra of perturbations and the validity of the consistency relations derived from the above analysis. We will also discuss the parameter ranges where the correlation of adiabatic and isocurvature perturbations is strong.

III. DOUBLE INFLATION WITH TWO MASSIVE SCALAR FIELDS

Let us first consider a simple model where massive scalar fields ϕ and χ are coupled through an interaction term $1/2 g^2 \phi^2 \chi^2$:

$$V(\phi,\chi) = \frac{1}{2}m_\phi^2\phi^2 + \frac{1}{2}m_\chi^2\chi^2 + \frac{1}{2}g^2\phi^2\chi^2. \tag{3.1}$$

There are three parameters associated with this potential: m_ϕ, m_χ, and g. Then there are four free parameters associated with the initial conditions of the fields: ϕ_i, χ_i, $\dot{\phi}_i$, and $\dot{\chi}_i$. Making use of the slow-roll approximation, $\dot{\phi} = -V_\phi/3H$ and $\dot{\chi} = -V_\chi/3H$ with $H^2 = (8\pi/3M_p^2)V$ in Eqs. (2.1) and (2.2), the initial conditions of $\dot{\phi}$ and $\dot{\chi}$ are determined by ϕ_i and χ_i.[4] This assumption cuts down the number of free parameters to two, ϕ_i and χ_i. Therefore we have five free parameters (m_ϕ, m_χ, g, ϕ_i, and χ_i) for the model (3.1). Once these parameters are given, the evolution of the background is determined, with the number of e-folds $N = -\ln(a/a_f)$, with a_f being the value of the scale factor at the end of inflation [13]. We shall introduce the number of e-folds N_H, which corresponds to the value of N when the scale corresponding to our Hubble radius today crossed out the Hubble radius during inflation. Hereafter we set it to be

$$N_H = 60, \tag{3.2}$$

in order to make definite calculations.

A. Noninteracting fields: $g = 0$

In the case where the fields are noninteracting ($g = 0$), the slow-roll approximation in Eqs. (2.1) and (2.2) gives the relation $\phi^2 + \chi^2 = 4N/\kappa^2$. The fields lie on a circle of radius $2\sqrt{N}/\kappa$. Therefore it is useful to write ϕ and χ in parametric form [13]:

$$\phi = \frac{2\sqrt{N}}{\kappa}\cos\alpha, \quad \chi = \frac{2\sqrt{N}}{\kappa}\sin\alpha. \tag{3.3}$$

This means that the evolution of two scalar fields is characterized by N and the scalar field position angle α, satisfying the relation $\tan\alpha = \chi/\phi$. The field velocity angle θ defined by Eq. (2.7) is related to α by

$$\tan\theta \simeq -\frac{2m_\chi^2\sqrt{N}}{3H\kappa\dot{\sigma}}\tan\alpha. \tag{3.4}$$

Making use of the relation (3.3), we find that the number of e-folds can be expressed as [13]

$$N = N_0 \frac{(\sin\alpha)^{2/(R^2-1)}}{(\cos\alpha)^{2R^2/(R^2-1)}}, \tag{3.5}$$

where

$$R \equiv m_\chi/m_\phi. \tag{3.6}$$

Note that the integration constant N_0 roughly corresponds to the number of e-folds during the second stage of inflation driven by the light scalar field. Hereafter we shall concentrate on the case where the field χ is heavier than ϕ, i.e., $R > 1$.

In order to know the evolution of the background we need to determine four parameters: m_ϕ, R, N_0, and α. When the total number of e-folds is fixed at around N_H, the model parameters are reduced to three (m_ϕ, R, and N_0). Whether inflation is dominated by the heavy or light fields when the scale of cosmological relevance crosses the Hubble radius depends on the value of N_0 relative to $N_H = 60$.

Adiabatic perturbations for modes larger than the Hubble radius during the radiation dominant era can be matched with the curvature perturbation at the end of inflation, which are given by [24,8]

[4] Clearly, assuming slow roll to set the initial conditions is not generally valid. Not assuming this will lead to extra transient violations of the slow-roll conditions, but if inflation is successfully initiated the fields should settle to their slow-roll values quickly. At any rate our interest is in correlations and violations of the slow-roll approximation in a minimal sense. Inverting CMB and LSS data to give information about the potential and initial conditions will have to deal with this possibility in general, however.

$$\mathcal{R} \simeq -\frac{\kappa^2 H(t_*)}{2\sqrt{2k^3}}[\phi(t_*)e_\phi(\mathbf{k}) + \chi(t_*)e_\chi(\mathbf{k})]$$
$$= -\frac{\kappa H(t_*)\sqrt{N}}{\sqrt{2k^3}}[\cos\alpha_* e_\phi(\mathbf{k}) + \sin\alpha_* e_\chi(\mathbf{k})], \tag{3.7}$$

where α_* is the value of α at the horizon crossing. Assuming that the field ϕ decays into ordinary matter (baryons, photons, neutrinos) and χ into cold dark matter, super-Hubble isocurvature perturbations during the radiation dominant era are expressed as [24,8]

$$S \simeq \frac{H(t_*)}{\sqrt{2k^3}}\left[R^2\frac{e_\phi(\mathbf{k})}{\phi(t_*)} - \frac{e_\chi(\mathbf{k})}{\chi(t_*)}\right]$$
$$= \frac{\kappa H(t_*)}{2\sqrt{N}\sqrt{2k^3}}\left[R^2\frac{e_\phi(\mathbf{k})}{\cos\alpha_*} - \frac{e_\chi(\mathbf{k})}{\sin\alpha_*}\right]. \tag{3.8}$$

The expression (3.7) indicates that for the adiabatic perturbation the heavy field χ dominates for $\tan\alpha_* > 1$, while the light field ϕ dominates for $\tan\alpha_* < 1$. From Eq. (3.8) we find that for the isocurvature perturbation the heavy field χ dominates for $\tan\alpha_* < 1/R^2$, while the light field ϕ dominates for $\tan\alpha_* > 1/R^2$.

Let us estimate the correlation r_C that is derived from the slow-roll analysis [see Eq. (2.39)]. This is not actually completely valid as we pointed out in the previous section, but useful to make a rough estimation for the correlation. We will check, of course, the validity of the analytic estimates by numerical simulations. By a simple calculation we find that x defined in Eq. (2.39) is given by

$$x = \frac{R^2(R^2-1)\tan\alpha_*(1+\tan^2\alpha_*)}{(1+R^2\tan^2\alpha_*)(1+R^4\tan^2\alpha_*)}\frac{1-e^{-\zeta_k N_k}}{\zeta_k N_k}. \tag{3.9}$$

If the condition $|\zeta_k|N_k \ll 1$ is satisfied, this reduces to

$$x = \frac{R^2(R^2-1)\tan\alpha_*(1+\tan^2\alpha_*)}{(1+R^2\tan^2\alpha_*)(1+R^4\tan^2\alpha_*)}. \tag{3.10}$$

Note that when $|\zeta_k|N_k \gtrsim 1$ one has $|(1-e^{-\zeta_k N_k})/(\zeta_k N_k)| \simeq 1/|(\zeta_k|N_k)| \lesssim 1$. Therefore the value of x is smaller than in the case of Eq. (3.10). Equation (2.38) implies that the correlation r_C vanishes for $x=0$ and gets larger for increasing x. In particular, when x is larger than of order unity, the correlation is strong (r_C is close to unity). From Eq. (3.9) we find that there is no correlation if the masses of the scalar fields are equal ($R=1$). We can also make a consistency check by using Eq. (3.9) or Eq. (3.10). When the masses of the scalar fields differ significantly ($R \to 0$ or $R \to \infty$), the correlation is also vanishingly small for fixed $\tan\alpha_*$.

In order to discuss the correlation precisely, it is useful to classify model parameters into three cases [24]: (1) $\tan\alpha_* \gg 1$, (2) $\tan\alpha_* \ll 1/R^2$, and (3) $1/R^2 < \tan\alpha_* < 1$. Hereafter we shall analyze the strength of the correlation as well as the power spectra and consistency relations, and check the validity of the slow-roll analysis.

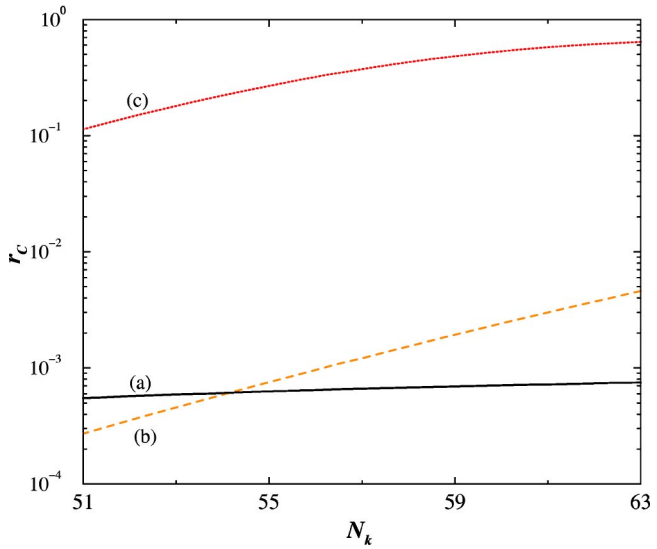

FIG. 1. Correlation spectra r_C for three different cases with $R=5$, $m_\phi = 2.0\times10^{-7}M_p$, and $g=0$. The cases correspond to (a) $\tan\alpha_* = 32.0 \gg 1$, (b) $\tan\alpha_* = 3.13\times10^{-4} \ll R^{-2}$, and (c) $R^{-2} < \tan\alpha_* = 0.16 < 1$, on the scale $N_k = 65$. Case (c) shows strong correlations, while the cases (a) and (c) do not.

1. $\tan\alpha_* \gg 1$

In this case the field χ is the main source for adiabatic perturbations, while isocurvature perturbations are dominated by the field ϕ. Therefore both perturbations are regarded as almost independent, and the correlation is weak (see Fig. 1). In fact, when $\tan\alpha_* \gg 1$, Eq. (3.10) yields

$$x \simeq \frac{R^2-1}{R^4}\frac{1}{\tan\alpha_*}. \tag{3.11}$$

Therefore the correlation r_C decreases with increasing $\tan\alpha_*$ and one has $r_C \to 0$ for $\tan\alpha_* \to \infty$. This decreasing rate is more significant for larger R as can be seen from Eq. (3.11) and Fig. 2.

The amplitude of isocurvature perturbations is not typically larger than that of adiabatic perturbations unless α_* is very close to $\pi/2$, as shown in Fig. 3.[5] Since the correlation term in Eq. (2.32) is neglected and $\epsilon_\phi \ll \epsilon_\chi$ for $\tan\alpha_* \gg 1$, one has a spectral index of the curvature perturbation that is approximately the same as in the single-field case:

$$n_\mathcal{R} - 1 \simeq -6\epsilon_\chi + 2\eta_{\chi\chi} = -\frac{1}{\pi}\left(\frac{M_p}{\chi}\right)^2. \tag{3.12}$$

This is a slowly red-tilted spectrum as found in Fig. 3. In Fig. 4 we plot the ratio r_T defined by Eq. (2.37) and its value obtained by the two consistency relations (2.41) and (2.42).

[5]Note, however, that the amplitude of isocurvature perturbations can be high if α_* is very close to $\pi/2$.

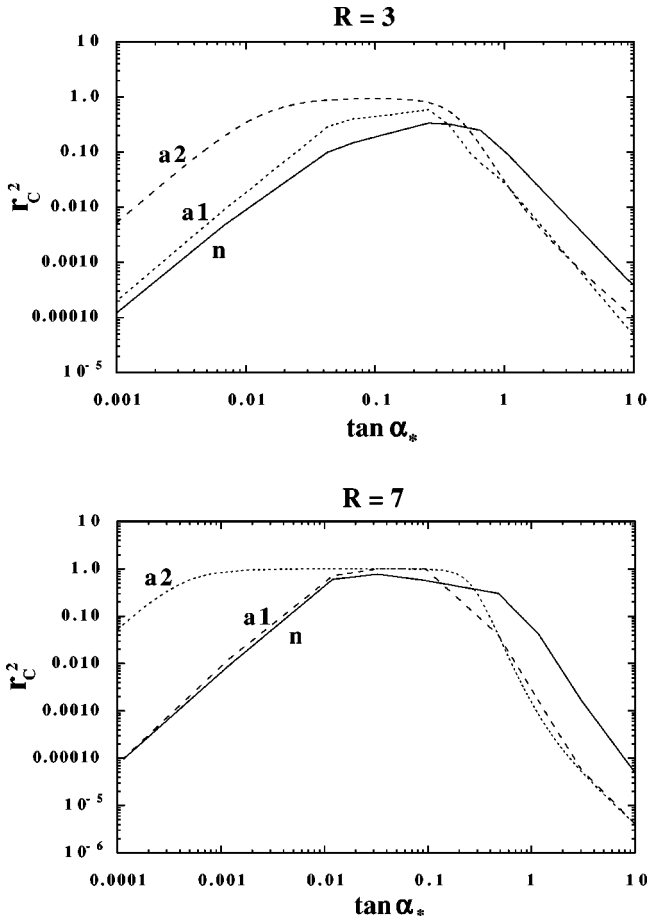

FIG. 2. The square of the correlation r_C as a function of $\tan\alpha_*$ for $R=3$ and $R=7$ with $m_\phi=2.0\times10^{-7}M_p$ and $g=0$ on a scale corresponding to $N_k=60$. The solid curve corresponds to the numerical result, while the dashed (a1) and dotted (a2) curves correspond to the results using Eqs. (3.9) and (3.10), respectively.

Except for some discontinuous behavior which accompanies the numerics,[6] the consistency relations show fairly good agreement with the value of the original definition of r_T. In this case, since r_C is much less than unity, the consistency relation (2.41) is essentially no different from that of the single-field case, $r_T=-n_T/2$; namely, it is almost the same as the single-field inflation driven by only one scalar field. Therefore the assumption that $\mu_Q^2/(3H^2)$, $\mu_s^2/(3H^2)$, and $\dot{\theta}/H$ do not vary too much during inflation can be justified in this case, thus not giving a strong deviation in the consistency relations.

2. $\tan\alpha_* \ll 1/R^2$

In this case the field ϕ is the main source for adiabatic perturbations, while isocurvature perturbations are dominated by the field χ. From Eq. (3.10) one has

[6]We evaluated the spectral indices numerically using the definition $n=1+\Delta(\ln P)/\Delta(\ln k)$, which leads to some numerical errors and some spikiness in some of the figures.

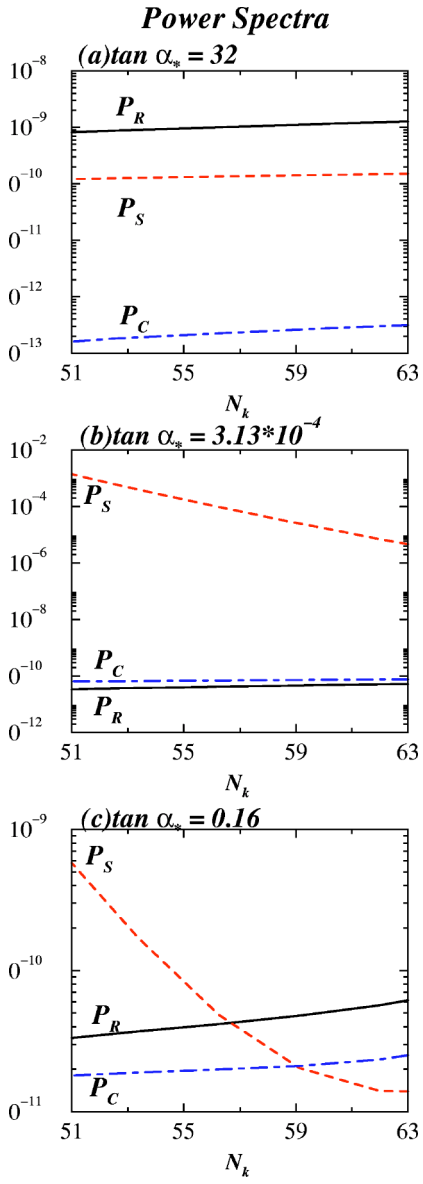

FIG. 3. The power spectra $P_{\mathcal{R}}$, P_S, and P_C with $R=5$, $m_\phi=2.0\times10^{-7}M_p$, and $g=0$. The curves correspond to the cases (a) $\tan\alpha_*=32.0\gg1$ (heavy-field dominated), (b) $\tan\alpha_*=3.13\times10^{-4}\ll R^{-2}$ (light-field dominated), and (c) $R^{-2}<\tan\alpha_*=0.16<1$, on a scale corresponding to $N_k=65$ (double inflation).

$$x\simeq R^2(R^2-1)\tan\alpha_* \tag{3.13}$$

for $R^2\tan\alpha_*\ll1$. Therefore adiabatic and isocurvature perturbations are almost independent of each other for smaller $\tan\alpha_*$, which can be confirmed in Fig. 1. In Fig. 2 we find that the prediction (3.10) overestimates the correlation ratio r_C when $\tan\alpha_*$ is small, while Eq. (3.9) shows fairly good agreement with the numerical results. This implies that $|\zeta_k|N_k$ could be larger than unity, in which case the $(1-e^{-\zeta_k{}^{N_k}})/(\zeta_k N_k)$ term cannot be neglected in Eq. (3.9).

When $\tan\alpha_*\ll1/R^2$ the amplitudes of isocurvature perturbations are larger than those of the adiabatic ones as predicted by Eqs. (3.7) and (3.8) (see Fig. 3). The spectrum of curvature perturbations is hardly affected by isocurvature

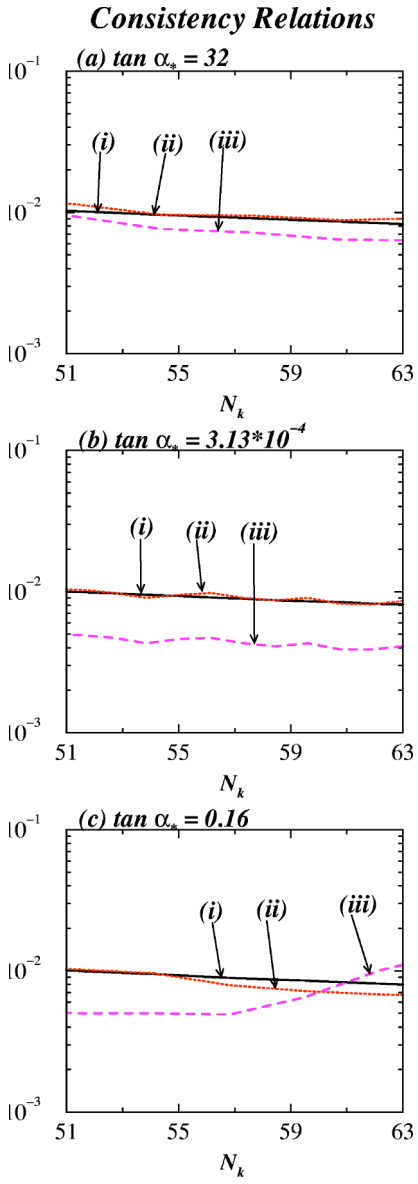

FIG. 4. The consistency relations with $R=5$, $m_\phi=2.0\times10^{-7}M_p$, and $g=0$. The curves correspond to the cases (a) $\tan\alpha_*=32.0\gg1$, (b) $\tan\alpha_*=3.13\times10^{-4}\ll R^{-2}$, and (c) $R^{-2}<\tan\alpha_*=0.16<1$, on a scale corresponding to $N_k=65$ (double inflation). The ratios r_T that are derived by using Eq. (2.36), and the two consistency relations Eqs. (2.41) and (2.42) are denoted by (i), (ii), and (iii), respectively. Note that while the r_T calculated numerically, (i), typically agrees with (ii), but it often differs from (iii).

perturbations because the correlation is small ($r_C\ll1$). Therefore the consistency relation in the single-field case should not be significantly modified in this case.

In fact, from Fig. 4 we find that the first consistency relation (2.41) shows good agreement with the original definition of r_T, while the second one (2.42) is not so good. Indeed, we should expect deviations from the predictions of the second consistency relation around the end of inflation because the masses of the adiabatic/entropy fields and $\dot\theta/H$ are not constant in this case. Even in case 1 the discrepancy in the second consistency relation is a bit larger than in the case of the first one.

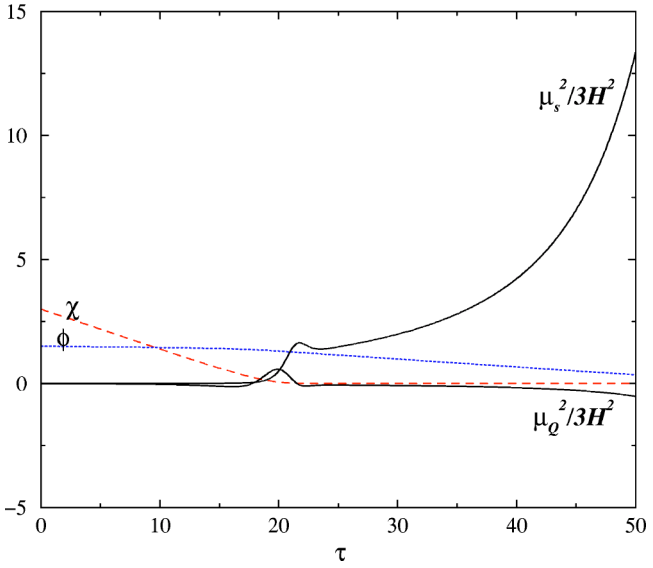

FIG. 5. The evolution of $\mu_Q^2/(3H^2)$ and $\mu_s^2/(3H^2)$ with $R=5$, $m_\chi=1\times10^{-6}M_p$, and $g=0$. The initial conditions are chosen to be $\chi=3M_p$ and $\phi=1.5M_p$. When the heavy field drops to the potential valley, a second phase of inflation begins, which is accompanied by an increase of $\mu_Q^2/(3H^2)$ and $\mu_s^2/(3H^2)$ The term $\mu_s^2/(3H^2)$ exhibits growth by a factor of 5×10^4 by the end of inflation compared to its initial value.

3. $1/R^2\leqslant\tan\alpha_*\leqslant1$

In this case both adiabatic and isocurvature perturbations are sourced by the light field ϕ, but the effect of the heavy field χ is also important. From Eq. (3.10) we find

$$x=\frac{(R^2-1)(R^4+1)}{2R^2(R^2+1)}\quad\text{for}\ \tan\alpha_*=\frac{1}{R^2}\qquad(3.14)$$

and

$$x=\frac{2R^2(R^2-1)}{(R^2+1)(R^4+1)}\quad\text{for}\ \tan\alpha_*=1.\qquad(3.15)$$

Therefore, when $\tan\alpha_*=1/R^2$ and R is not too close to unity, x is typically larger than unity (for example, one has $x>1.275$ for $R>2$). In this case the correlation ratio r_C is close to 1. The range of this high correlation gets wider for larger R as found in Fig. 2. When $\tan\alpha_*\simeq1$, x is at a maximum, $x_{\max}\simeq0.3$ for $R\simeq1.7$, with the correlation ratio range $r_C\leqslant0.28$ in this case. As R is increased, the maximum correlation becomes smaller, as is seen in Fig. 2.

Note that we need to include the correction term $(1-e^{\zeta_k N_k})/(\zeta_k N_k)$ in Eq. (3.9) to accurately estimate the strength of the correlation. Figure 2 clearly indicates that the correlation is strong around $1/R^2\leqslant\tan\alpha_*\leqslant1$. In this case the correlation term r_C^2 is very important in the consistency relation (2.41) because r_C will be close to unity.

As found from Fig. 2 analytic estimates by slow-roll approximations typically give larger values of r_C around the region where the correlation is strong. When r_C is close to unity, this difference can affect the consistency relation (2.41). In Figs. 5 and 6 we plot the evolution of $\mu_Q^2/(3H^2)$,

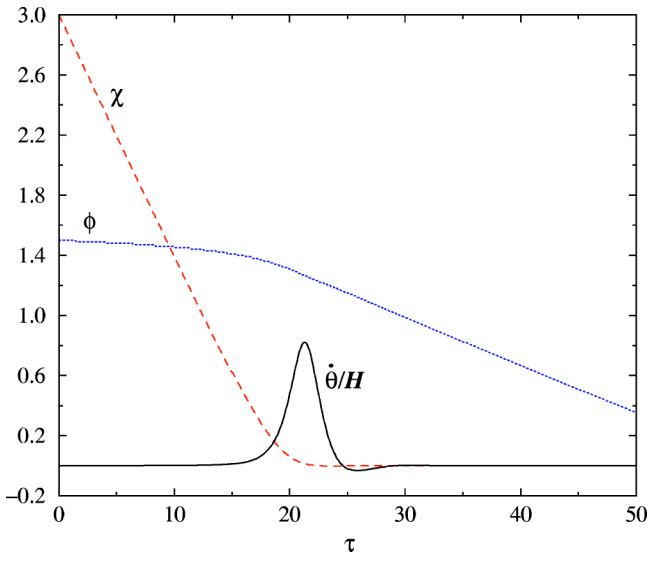

FIG. 6. The evolution of $\dot{\theta}/H$ with the same initial conditions as in Fig. 5. When the heavy field drops to the potential valley, a second phase of inflation begins, which is accompanied by an increase of $\dot{\theta}/H$ from the initial value 1.44×10^{-3} to its peak value $\dot{\theta}/H=0.8$ around the end of the first stage of inflation.

$\mu_s^2/(3H^2)$, and $\dot{\theta}/H$ for $R=5$, $m_\chi=1\times10^{-6}M_p$, and $g=0$ with initial conditions $\chi=3M_p$ and $\phi=1.5M_p$. The heavy field χ leads to the first phase of inflation until $\tau\equiv10^{-6}M_pt\simeq20$, which is followed by the second stage of inflation driven by ϕ. All of $\mu_Q^2/(3H^2)$, $\mu_s^2/(3H^2)$, and $\dot{\theta}/H$ exhibit a rapid increase around the end of the first stage of inflation due to the breakdown of the slow-roll conditions for χ. For example, $\mu_s^2/(3H^2)$ continues to grow by the end of the second stage of inflation, whose growth is about 5×10^4 times its initial value.

In this case the assumption of the constancy of the mass terms is no longer justified in Eqs. (2.17) and (2.21), thereby leading to errors in the correlation r_C if we use the estimation in Eq. (2.39). In addition, the peak value of $\dot{\theta}/H$ typically provides a larger contribution than its value at horizon crossing in Eq. (2.39). Therefore we need to evaluate the values of x and r_C numerically in order to estimate the correlation accurately.

In the case where the correlation is strong at horizon crossing, we expect to find some deviations even from the predictions of the first consistency relation. In fact the numerical result in Fig. 4(c) does not completely agree with the slow-roll results, although the deviation is not significant. This case corresponds to the one where the slow-roll conditions are violated at horizon crossing. We have numerically checked that the first consistency relation holds well as long as the slow-roll conditions are satisfied at horizon crossing, which agrees with the claim by Wands *et al.* [34]. The second consistency relation is more strongly affected by the violation of the slow-roll conditions during double inflation, especially when the correlation is strong. The slow-roll analysis shows some limitations to correctly estimate three spectral indices $n_{\mathcal{R}}$, n_S, and n_C. Numerical analysis is required as well in order to fully understand the strength of the correlation and the final power spectra of adiabatic and isocurvature perturbations.

In Fig. 1 we find that the correlation is high around $N_k\gtrsim60$, and decreases toward smaller scales. This corresponds to the "light" inflationary phase with $\theta\lesssim1/R$ where the perturbations are mainly sourced by the field ϕ around $N_k\simeq60$. In this case the correlation gets weaker toward smaller scales due to the decrease of $\dot{\theta}$. If the scale $N_k=60$ corresponds to the "heavy" inflationary phase with $\alpha\gtrsim1/R$, the correlation r_C is nearly constant as shown in Ref. [24]. This means that α varies slowly during the heavy field inflation, which makes $\dot{\theta}$ unsuppressed. The slow variation of r_C can actually be found in case (a) of Fig. 1. Note that if we choose a value of α not much greater than $1/R$ the correlation can be higher as claimed in Ref. [24].

Two important quantities to determine the strength of the correlation are R and $\tan\alpha_*$ around $N_H\simeq60$ as seen from Eq. (3.9). The e-folding of the second stage of inflation, N_0, determines whether inflation is dominated by a heavy or light scalar field around $N_H\simeq60$ and also the strength of the correlation on smaller scales. Either of the scalar field masses m_ϕ or m_χ can be determined by the Cosmic Background Explorer (COBE) normalization. The ratio $R=m_\chi/m_\phi$ is important when we discuss the correlation r_C. The correlation is strong around $1/R^2\leqslant\tan\alpha_*\leqslant1$, whose lower bound is also determined by R. If precise observations in the future reveal the strength of the correlation around $50\lesssim N_k\lesssim63$, we will be able to constrain two masses m_ϕ and m_χ (alternatively R and m_ϕ) together with the values of $\tan\alpha_*$ and N_0.

B. The interacting case: $g\neq0$

Let us next consider the case where the coupling g is taken into account. It was suggested by Linde and Mukhanov [18] that inclusion of the coupling g can lead to a blue spectrum of isocurvature perturbations. Here we shall make a detailed analysis of the correlation of adiabatic and isocurvature perturbations.

Let us first estimate the spectrum of isocurvature perturbations using the analytic estimates of Sec. II. Although it has some errors due to the breakdown of the slow-roll approximation, it is still useful to make rough estimates for the power spectrum. The spectral index in Eq. (2.33) is estimated as

$$n_S-1=-2\epsilon_t+\frac{2\mu_s^2}{3H^2}. \tag{3.16}$$

Therefore it is important to consider the mass of the entropy field perturbation μ_s relative to the Hubble rate H. Note that the term $-2\epsilon_t$ in the RHS of Eq. (3.16) provides the slowly red-tilted spectrum. If the mass square μ_s^2 is larger than of order H^2, isocurvature perturbations are blue tilted with $n_S>1$. Making use of the slow-roll result (2.18), we find

$$\frac{2\mu_s^2}{3H^2}=\frac{4(m_\chi^2+g^2\phi^2)(m_\phi^2+g^2\chi^2)(m_\phi^2\phi^2+m_\chi^2\chi^2-2g^2\phi^2\chi^2)}{\kappa^2(m_\phi^2\phi^2+m_\chi^2\chi^2+g^2\phi^2\chi^2)\{(m_\phi^2+g^2\chi^2)^2\phi^2+(m_\chi^2+g^2\phi^2)^2\chi^2\}}. \tag{3.17}$$

Let us first consider the case where μ_s^2 is positive during the whole stage of double inflation, which corresponds to the condition $m_\phi^2\phi^2+m_\chi^2\chi^2>2g^2\phi^2\chi^2$. When the heavy field χ rolls down to the valley $\chi=0$ at the first stage of inflation, we have $\mu_s^2\simeq m_\chi^2+g^2\phi^2$ and $3H^2\simeq 4\pi m_\phi^2\phi^2/M_p^2$. Then the mass square of δs is given by

$$\mu_s^2\simeq m_\chi^2+\beta H^2 \quad \text{with} \quad \beta=\frac{3g^2}{4\pi}\left(\frac{M_p}{m_\phi}\right)^2. \tag{3.18}$$

Note that in this case the entropy field perturbation δs is almost the same as the heavy field perturbation $\delta\chi$. If χ is quickly suppressed, we need to consider only $\delta\chi$, as in Ref. [18], in order to discuss the spectrum of isocurvature perturbations. When βH^2 is larger than m_χ^2 during double inflation, we have $\mu_s^2\simeq\beta H^2$ and

$$n_S-1\simeq -2\epsilon_t+\frac{2}{3}\beta. \tag{3.19}$$

When β is much larger than unity, this yields the blue-tilted spectrum, $n_S>1$.[7] Making use of this scenario, it is possible to obtain isocurvature perturbations that tend to grow toward smaller scales while adiabatic perturbations remain small on present horizon scales [18]. If $\mu_s^2\gg H^2$, then χ rolls down very rapidly to the local minimum of the potential valley ($\chi\to 0$), and $\dot\theta$ in Eq. (2.30) exponentially decreases on smaller scales. In this case the correlation between adiabatic and isocurvature perturbations tends to be very weak except for the scales where χ is not very small compared to ϕ. When $\dot\theta$ is negligible, the spectrum of curvature perturbations is essentially no different from the single-field result, $n_{\mathcal{R}}-1=-6\epsilon_\phi+2\eta_{\phi\phi}$ [see Eq. (2.32)]. In this case adiabatic perturbations can be nearly scale invariant, while isocurvature perturbations are blue tilted.

From Eq. (3.18) we find that the spectrum of isocurvature perturbations can be blue tilted for the coupling g with $g\gtrsim m_\phi/M_p$. In Fig. 7 we plot the spectra of $P_{\mathcal{R}}$, P_S, and P_C for two cases with $\beta=0.01$ and 0.95. Note that in these cases the model parameters are chosen so that μ_s^2 is positive during the whole of double inflation. When $\beta=0.01$, the spectrum of isocurvature perturbations is slightly blue tilted, while for $\beta=0.95$ it is highly blue tilted.

The two spectra $P_{\mathcal{R}}$ and P_C are not significantly modified by the presence of the coupling term g. It can be understood that the correlation of adiabatic and isocurvature perturbations gets smaller as χ approaches the potential valley with decreasing $\dot\theta$. As shown in Fig. 8 the correlation r_C tends to decrease more on smaller scales as we choose larger values of β. When $\beta\gtrsim 1$ we find that r_C decreases rapidly on smaller scales, which is associated with the highly blue-tilted spectrum of isocurvature perturbations. This is confirmed by the definition of r_C in Eq. (2.36) where only P_S increases toward smaller scales.

From Fig. 8 we find that the first consistency relation (2.41) exhibits fairly good agreement with r_T obtained by Eq. (2.37) except for larger scales, while the second one (2.41) does not. This is caused by the violation of the slow-roll conditions at horizon crossing and also by the change of $\mu_Q^2/(3H^2)$, $\mu_s^2/(3H^2)$, and $\dot\theta/H$ during inflation. Since the correlation decreases toward smaller scales, the deviation from the numerical results tends to be weaker for smaller N_k in the case of the first consistency relation. Since the second consistency relation is affected by the change of the mass terms after horizon crossing, it does not agree well with the numerical results even on smaller scales.

Note that in Fig. 8 the strength of the correlation r_C increases for larger β around the scale $N_H=60$. Since the inclusion of the coupling g provides the additional source term

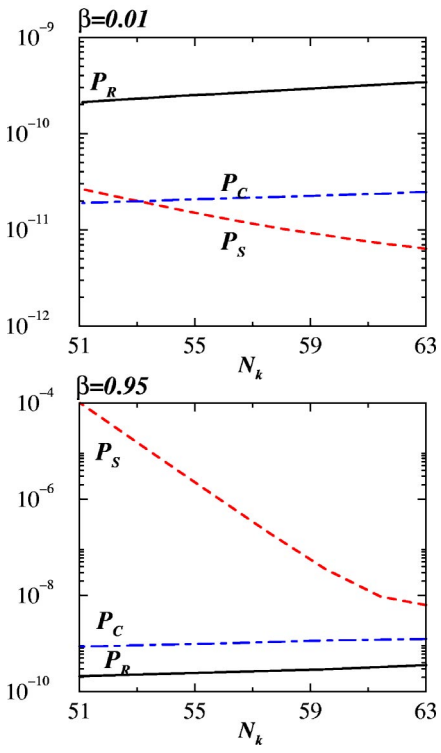

FIG. 7. The power spectra $P_{\mathcal{R}}$, P_S, and P_C are shown for $\beta=0.01$ and 0.95. The model parameters are chosen to be $R=3$, $m_\phi=5.0\times 10^{-7}M_p$, and $\phi=3.2M_p$, $\chi=0.3M_p$ at $N_k=65$.

[7]When $\beta\gg 1$ the spectrum of isocurvature perturbations is highly blue tilted. This is actually the case for the preheating scenario where large-scale entropy field perturbations are strongly suppressed for the coupling g required for strong preheating (see Refs. [36]).

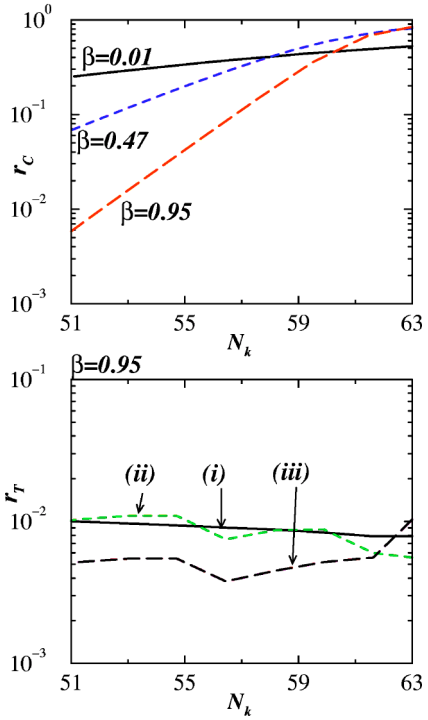

FIG. 8. The correlation r_C for $\beta=0.01$, 0.47, 0.95 and the ratio r_T which is derived by Eqs. (2.37), (2.41), and (2.42), denoted by (i), (ii), and (iii), respectively. The model parameters are chosen to be the same as in Fig. 7.

for $\dot{\theta}$ [see the $\eta_{\phi\chi}$ term in Eq. (2.23)], this works to induce a larger correlation as long as χ is not strongly suppressed. Making use of Eq. (2.23), we can easily show that the correlation is nonzero even for $R=1$.[8] Figure 9 indicates that the values of r_C are increased around the region where the correlation is strong by including the coupling g.

If the condition $m_\phi^2\phi^2+m_\chi^2\chi^2<2g^2\phi^2\chi^2$ is satisfied at horizon crossing, the mass of δs is *negative*. So the spectrum of isocurvature perturbations produced is red tilted with a steeper slope than in the case of $g=0$. Figure 10 corresponds to the case where the spectrum P_S is red tilted for $57\lesssim N_k \lesssim 63$ but begins to be blue tilted for $N_k\lesssim 57$. The negative mass of δs leads to a red-tilted spectrum on large scales as expected. When ϕ and χ are of the same order on these scales, the correlation r_C can be close to unity (see the right panel of Fig. 10). When the mass of δs becomes positive and χ begins to decrease toward $\chi=0$, the situation is almost the same as discussed previously. In this case we have a highly blue-tilted spectrum for isocurvature perturbations with suppressed correlations ($r_C\ll 1$).

Unless g is extremely small ($g\ll m_\phi/M_p$), then it is natural to have a stage of negative μ_s^2 during double inflation. For example, when $g\gtrsim m_\phi/M_p$, it is easy to satisfy the condition $\mu_s^2<0$ if χ is larger than the order of the Planck mass. For the double-inflationary scenario where inflation starts out with large initial values of ϕ and χ much greater than the

[8]We have $r_C=0$ for $R=1$ and $\phi=\chi$.

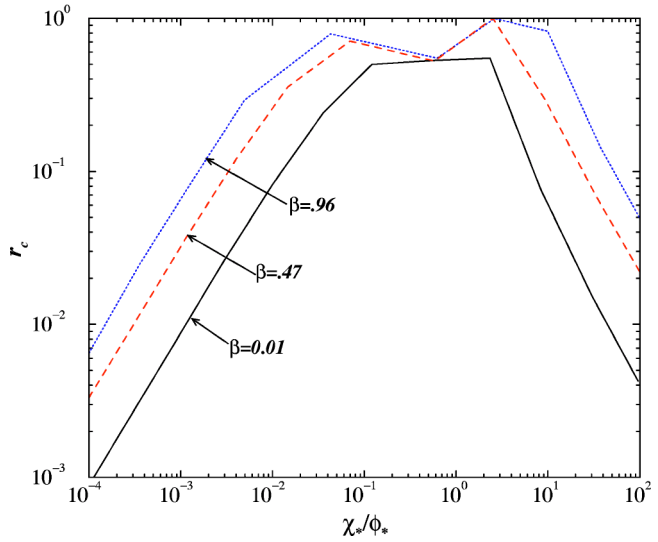

FIG. 9. The correlation r_C as a function of χ_*/ϕ_* for $\beta=0.01,0.47,0.95$ on a scale corresponding to $N_k=60$. The model parameters are the same as in Fig. 7.

Planck mass, the spectrum P_S is highly red tilted. Nevertheless, when g is large and $\beta\gg 1$, χ decreases very rapidly toward $\chi=0$. Therefore the blue-tilted spectrum of P_S appears immediately once the mass of δs becomes positive.

We have found that a variety of power spectra and correlations can be obtained, depending on the initial values of the scalar fields and the parameters of the model. In particular, the inclusion of the coupling g leads to an interesting power

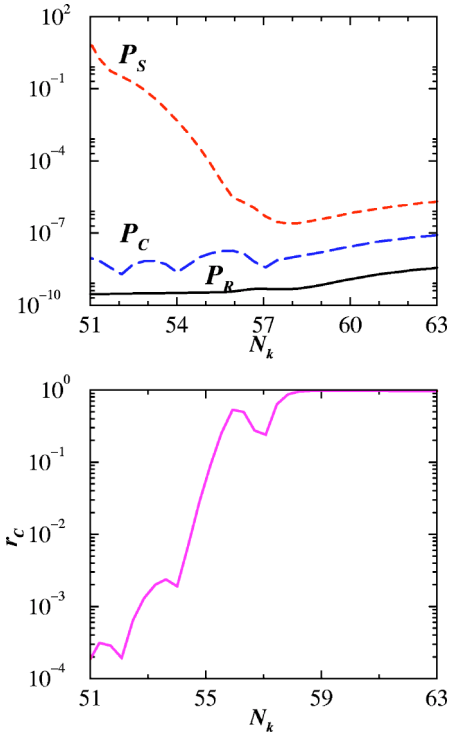

FIG. 10. The power spectra $P_{\mathcal{R}}$, P_S, P_C (top) and the correlation r_C (bottom) for $R=3$, $m_\phi=2.0\times 10^{-7}M_p$, and $g=2.0\times 10^{-6}$ (corresponding to $\beta=23.9$).

spectrum of isocurvature perturbations that tend to increase toward large scales (corresponding to $\mu_s^2<0$) and also grow again toward smaller scales (corresponding to $\mu_s^2>0$). If such a spectrum is supported by observations, it should be possible to constrain the strength of the coupling g and other model parameters by taking into account the information on the correlation r_C as well.

There exist other models of double inflation which provide the βH^2 correction as in Eq. (3.18). One such model is a nonminimally coupled χ field with a minimally coupled field ϕ [18]:

$$V=\frac{1}{2}m_\phi^2\phi^2+\frac{1}{2}m_\chi^2\chi^2+\frac{1}{2}\xi R\chi^2, \tag{3.20}$$

where ξ is a nonminimal coupling between the scalar curvature R and the field χ. In this model the spectrum of the isocurvature perturbations is red tilted due to the amplification of $\delta\chi$ for negative ξ [28,32], while it is blue tilted for positive ξ. Although the decomposition into adiabatic and entropy ''fields'' is not as simple as in the case of minimally coupled fields discussed in Sec. II, it would be of interest to extend our analysis to this case.

IV. DOUBLE INFLATION MOTIVATED BY SUPERSYMMETRY

We now come to perhaps the most interesting of the models we have studied. In hybrid and supernatural inflationary models [43–45], the symmetry breaking transition occurs in the presence of the second scalar field χ. The effective potential of the original hybrid inflation model is given by [43]

$$V=\frac{\lambda}{4}\left(\chi^2-\frac{M^2}{\lambda}\right)^2+\frac{1}{2}g^2\phi^2\chi^2+\frac{1}{2}m^2\phi^2. \tag{4.1}$$

This potential is closely related to those obtained in supersymmetric theories [45–51]. For example, consider the supersymmetric theory with a superpotential

$$W=S(\kappa_0\varphi\bar{\varphi}-\mu^2), \tag{4.2}$$

which includes two superfields S,φ together with a conjugate pair $\bar{\varphi}$. In the global supersymmetric limit ($M_p\to\infty$), one obtains the following effective potential for two superfields S and φ:

$$V=|\kappa_0\varphi\bar{\varphi}-\mu^2|^2+\kappa_0^2|S|^2(|\varphi|^2+|\bar{\varphi}|^2)+D \text{ terms}. \tag{4.3}$$

Note that this has a potential minimum at $|S|=0$, $\langle\varphi\rangle\langle\bar{\varphi}\rangle=\mu^2/\kappa_0$, $|\langle\varphi\rangle|=|\langle\bar{\varphi}\rangle|$. Making gauge and R transformations in the D-flat direction $|\langle\varphi\rangle|=|\langle\bar{\varphi}\rangle|$, the complex superfields $S,\varphi,\bar{\varphi}$ can be replaced by real scalar fields ϕ and χ as

$$S=\phi/\sqrt{2},\quad \varphi=\bar{\varphi}=\chi/2. \tag{4.4}$$

Then the potential (4.3) yields

$$V=\frac{\kappa_0^2}{16}\left(\chi^2-\frac{4\mu^2}{\kappa_0}\right)^2+\frac{1}{4}\kappa_0^2\phi^2\chi^2, \tag{4.5}$$

where we neglected the D terms. The absolute minimum appears at $\phi=0$, $\chi=2\mu/\sqrt{\kappa_0}$. The potential (4.5) is exactly flat at the local minimum $\chi=0$. Adding a mass term $1/2m^2\phi^2$ in Eq. (4.5) results in the effective potential (4.1) with the replacements $\kappa_0^2/2=g^2=2\lambda$ and $\mu^2=M^2/(2\sqrt{\lambda})$. Therefore the supersymmetric version of the hybrid or double inflation corresponds to the case with $g^2/\lambda=2$.

Taking into account the supergravity correction gives rise to a slowly varying effective potential, whose form is approximately given by $V\simeq\mu^4[1+\phi^4/(8M_p^4)]$ [50]. If one-loop radiative corrections are included, the total effective potential for $\phi>\sqrt{2}\mu/\sqrt{\kappa_0}$ involves a logarithmic term $\ln\phi$, as well as the ϕ^4 term [51]. The correction terms ϕ^4 or $\ln\phi$ can lead to an inflationary expansion of the universe for $\phi>\sqrt{2}\mu/\sqrt{\kappa_0}$.

Although these are different from the mass term $1/2m^2\phi^2$ in Eq. (4.1), the basic structures of the models motivated by supersymmetric theories are well described by the potential (4.1). In particular, when we discuss the correlation between adiabatic and isocurvature perturbations, the crucial point is the evolution of scalar fields *after* the symmetry breaking phase rather than the early evolution at $\phi>\sqrt{2}\mu/\sqrt{\kappa_0}$. Therefore we shall consider the model (4.1) in order to understand the basic properties of the correlations. We are particularly interested in the supersymmetric case with $g^2/\lambda=2$.

A. The condition for double inflation and the background evolution

We shall first consider the evolution of the background and the condition for double inflation to take place (rather than just a single phase of inflation) for the model (4.1). When ϕ is larger than $\phi_c\equiv M/g$, inflation takes place due to the slow-roll evolution of ϕ. Since the mass of χ is positive for $\phi>\phi_c$, the field χ rolls down to the potential valley at $\chi=0$. Therefore the potential is approximately described as $V\simeq M^4/4\lambda+(1/2)m^2\phi^2$. If the condition $m^2\phi_c^2\ll M^4/\lambda$ is satisfied, the Hubble constant at $\phi=\phi_c$ is given by $H\simeq H_0\equiv\sqrt{2\pi/(3\lambda)}M^2/M_p$. Let us denote the masses of the two fields ϕ and χ relative to H_0^2 as γ and δ:

$$\gamma\equiv\frac{m^2}{H_0^2}=\frac{3\lambda m^2M_p^2}{2\pi M^4},$$

$$\delta\equiv\frac{g^2\phi^2-M^2}{H_0^2}=\frac{3\lambda}{2\pi}\left(\frac{M_p}{M}\right)^2(c^2-1), \tag{4.6}$$

where we set $\phi=c\phi_c$. γ is required to be smaller than unity in order to lead to the first stage of inflation for $\phi>\phi_c$, thereby yielding

$$M^2\gtrsim mM_p\sqrt{\lambda}. \tag{4.7}$$

Whether the second stage of inflation occurs or not after ϕ drops below ϕ_c depends on the model parameters. If the ''waterfall'' condition

$$M^3\ll\lambda mM_p^2 \tag{4.8}$$

is satisfied, inflation soon comes to an end after the symmetry breaking. This corresponds to the original version of the hybrid inflationary scenario where inflation ends due to the rapid rolling of the field χ [43].

Combining Eqs. (4.7) and (4.8), one has $M \gg m$ and

$$\delta \gg \frac{M}{m}(c^2-1) \gg c^2-1. \tag{4.9}$$

This means that the classical field χ is strongly suppressed for $\phi > \phi_c$ ($\chi \propto a^{-3/2}$). Since inflation typically starts when the value of c^2-1 is of order unity or much larger than unity, it is inevitable to avoid the suppression of χ when the waterfall condition is satisfied. Note that δ changes sign after the symmetry breaking. The field χ and its large-scale fluctuations are amplified by the tachyonic instability associated with negative χ mass [56–59].

Although the growth is strong for large-scale modes ($k \to 0$), the size of these fluctuations is vanishingly small at the beginning of the tachyonic instability due to their exponential suppression for $\phi > \phi_c$. Therefore the small-scale modes that are not significantly suppressed for $\phi > \phi_c$ provide the larger contribution to the total variance $\langle \chi^2 \rangle$ of χ rather than the large-scale modes.

The condition for the second stage of inflation to occur is characterized by $|\delta| \ll 1$, namely,

$$M^2 \gg \lambda M_p^2. \tag{4.10}$$

In this case the field χ and its large-scale perturbation are free from the inflationary suppression for $\phi > \phi_c$, unless inflation starts out with very large values of ϕ satisfying $c \gg 1$. Note that one has $m^2/M^2 \ll g^2/\lambda$ under the condition that the first stage of inflation is driven by the Hubble constant H_0 (namely, $m^2\phi_c^2 \ll M^4/\lambda$).

Therefore one has $M \gg m$ for $g^2/\lambda = \mathcal{O}(1)$. Combining this relation with Eq. (4.10) gives $M^3 \gg \lambda m M_p^2$, which means that the waterfall condition (4.8) is violated. In this case the evolution of the field χ is sufficiently slow so that the second stage of inflation occurs after the symmetry breaking.

Let us consider the evolution of the background for $g^2/\lambda = \mathcal{O}(1)$. The number of e-folds during the first stage of inflation is described as

$$N_1 \simeq \kappa^2 \int_{\phi_c}^{\phi_i} \frac{V}{V'} d\phi \simeq \frac{2\pi M^2}{\lambda m^2 M_p^2} \ln \frac{\phi_i}{\phi_c}, \tag{4.11}$$

where we used $V \simeq M^4/4\lambda + (1/2)m^2\phi^2$ for $\phi > \phi_c$. Here ϕ_i is the value of ϕ at the beginning of double inflation. Note that we have $N_1 \gg 1$ under the condition of Eq. (4.7) (i.e., $\gamma \ll 1$). Similarly, the number of e-folds after the symmetry breaking is approximately expressed as

$$N_2 \simeq \kappa^2 \int_{\chi_0}^{\chi_c} \frac{V}{V'} d\chi \simeq \frac{2\pi M^2}{\lambda M_p^2} \ln \frac{\chi_0}{\chi_c}, \tag{4.12}$$

where we used $V \simeq (\lambda/4)(\chi^2 - M^2/\lambda)^2$. Here $\chi_0 = M/\sqrt{\lambda}$ and χ_c is the value of χ at $\phi = \phi_c$. Again $N_2 \gg 1$ is satisfied under the condition of Eq. (4.10). We are interested in the double-inflationary scenario where the total number of e-folds, $N_T = N_1 + N_2$, exceeds $N_H = 60$.

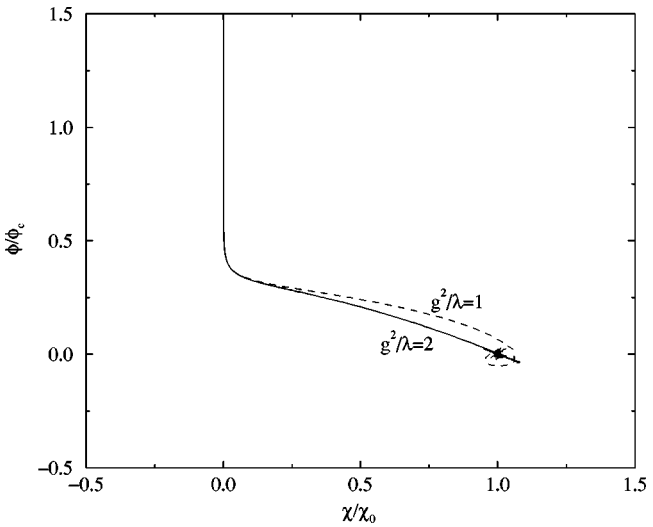

FIG. 11. The trajectory of two scalar fields in the plane $(\phi/\phi_c, \chi/\chi_0)$. The model parameters are chosen to be $M = 7.0 \times 10^{-7} M_p$, $m = 2.0 \times 10^{-7} M_p$ with initial scalar fields $\phi_i = 1.5\phi_c$ and $\chi_i = 10^{-3}\chi_0$. We show two cases of $g^2/\lambda = 1$ and 2 with $\lambda = 10^{-12}$. The trajectories are curved in field space, which means that $\dot{\theta} \neq 0$.

When $g^2/\lambda = \mathcal{O}(1)$, the critical value $\phi_c = M/g$ and the potential minimum $\chi_0 = M/\sqrt{\lambda}$ are of the same order. The two fundamental masses around the potential minimum are characterized by $m_\phi \equiv (g/\sqrt{\lambda})M$ and $m_\chi \equiv \sqrt{2}M$. Therefore these masses are also comparable when $g^2/\lambda = \mathcal{O}(1)$. In particular, in the supersymmetric case with $g^2/\lambda = 2$, the two masses are completely equal.

In this case the trajectory of the two scalar fields after the symmetry breaking is close to a straight line in the $(\phi/\phi_c, \chi/\chi_0)$ plane if the velocities of ϕ and χ are sufficiently small at the bifurcation point $\phi = \phi_c$ [60]. However, since $\dot{\phi}$ is nonzero because of the non-slow-roll evolution around $\phi = \phi_c$, the trajectory is not strictly described by a straight line after the symmetry breaking. In fact this behavior can be found in our numerical simulation in Fig. 11. When $g^2/\lambda = \mathcal{O}(1)$ and $g^2/\lambda \neq 2$ the two scalar fields exhibit chaotic behavior as shown in Refs. [60–62]. The trajectory in the $g^2/\lambda = 1$ case is illustrated in Fig. 11.[9] Since the trajectory of the two scalar fields is generally curved, this leads to a variation of θ in field space ($\dot{\theta} \neq 0$), thereby generating a correlation of perturbations for $\phi < \phi_c$. Note that in the case of $g^2/\lambda \ll 1$ or $g^2/\lambda \gg 1$, m_ϕ and m_χ as well as ϕ_c and χ_0 take quite different values. We will not consider such cases in this work, since we are interested in the double inflation motivated by supersymmetric theories.

B. Perturbations

Let us next analyze the perturbations and correlations in the double inflation model with the potential (4.1). When the

[9]Note that the amplitude of the two scalar fields can be higher, as in Refs. [62,60] by changing the model parameters.

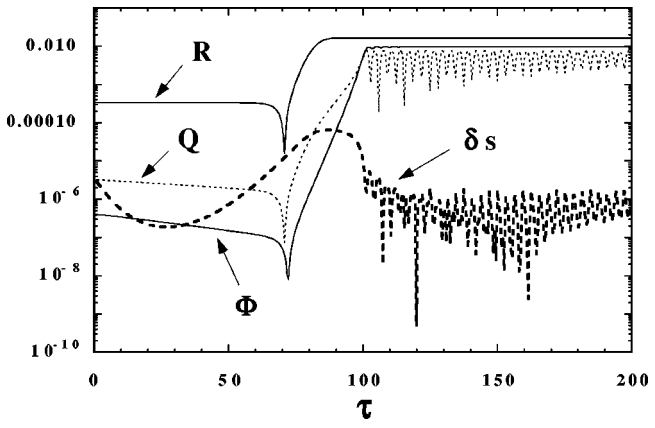

FIG. 12. The evolution of $\mathcal{R}$, Φ, $\dot{\delta}_s$, and Q for a mode that left the horizon before 60 e-foldings from the end of the double inflation. Note that we showed $\mathcal{R}=\sqrt{P_{\mathcal{R}}}$, etc. The model parameters are $g^2/\lambda=2$, $g=1.5\times10^{-10}$, $M=5.0\times10^{-6}$, and $m=0.2M$ with initial conditions $\phi=1.34\phi_c$ and $N=10^{-3}\chi_0$. $\mathcal{R}$ and Φ are amplified due to the tachyonic growth of δs and Q during the second stage of inflation.

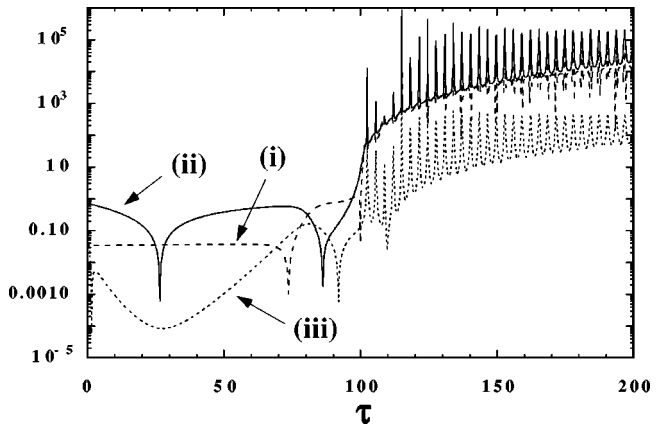

FIG. 13. The evolution of (i) $|\mu_Q^2/(3H^2)|$, (ii) $|\mu_s^2/(3H^2)|$, and (iii) $|\dot{\theta}/H|$ for $g^2/\lambda=2$, $g=1.5\times10^{-10}$, $M=5.0\times10^{-6}$, and $m=0.2$ M with initial conditions $\phi=1.34\phi_c$ and $\chi=10^{-3}\chi_0$. Although we showed the absolute values of these quantities, it happens that these take negative values in the tachyonic instability region.

field ϕ evolves slowly along the potential valley with $\chi=0$ before the symmetry breaking, the spectral index of the curvature perturbation generated in the first stage of double inflation can be estimated by Eq. (2.32) as

$$n_{\mathcal{R}}-1\simeq-6\epsilon_\phi+2\eta_{\phi\phi}\simeq\frac{2}{3}\gamma\left(1-\frac{3m^2\phi^2}{V}\right), \quad (4.13)$$

where γ is defined by Eq. (4.6). When the condition $m^2\phi^2 \ll V\simeq M^4/(4\lambda)$, holds as is the case with the original hybrid inflation scenario [43], one has the blue-tilted spectrum with $n_{\mathcal{R}}-1\simeq(2/3)\gamma>0$. Similarly, the spectral index of the isocurvature perturbation generated for $\phi>\phi_c$ is given by

$$n_S-1\simeq-2\epsilon_\phi+2\eta_{\chi\chi}\simeq\frac{2}{3}\delta-\gamma\frac{m^2\phi^2}{3V}, \quad (4.14)$$

where we used Eq. (2.33). Therefore, when the condition $(2/3)\delta>\gamma m^2\phi^2/3V$ is satisfied, the isocurvature perturbation is also blue tilted. Note that the spectral index of the correlation P_C is similar to that of P_S except for the last term in Eq. (2.34), which is of order $1/N_k\ll1$ when $|\zeta_k N_k|\ll1$.

The spectral indices in Eqs. (4.13) and (4.14) can be modified in the presence of the tachyonic instability region with $\phi<\phi_c$. After the symmetry breaking, the field perturbation $\delta\chi$ begins to be amplified due to the negative χ mass in Eq. (4.6) with $c<1$. This growth is accompanied by the amplification of the entropy field perturbation δs for small k modes, which stimulates the enhancement of large-scale curvature perturbations by the relation (2.25) (see Fig. 12).

As shown in Fig. 13, $|\dot{\theta}/H|$ decreases during the first stage of inflation, but begins to increase after the symmetry breaking. This can lead to the strong correlation between adiabatic and isocurvature perturbations. In fact once δs and $|\dot{\theta}/H|$ grow sufficiently, they work as source terms for Q in the RHS of Eq. (2.14), thereby stimulating the growth of Φ through the relation (2.12). This behavior is clearly seen in the numerical simulation of Fig. 12.

Let us consider the spectra of perturbations at the end of double inflation. In Fig. 14 we show the spectra $P_{\mathcal{R}}$, P_S, and P_C around the scale $N_H=60$ for three different cases. The case (a) corresponds to the one with $\gamma\simeq0.08\ll1$ and $\delta\simeq c^2-1\simeq1$ around $N_k\sim60$, in which case from Eqs. (4.13) and (4.14) one has a slight blue tilt for $P_{\mathcal{R}}$ and a rather steep blue tilt for P_S at the end of the *first* stage of the double inflation.

In fact we have numerically checked that such spectra are generated before symmetry breaking. However, these are different from the final spectra obtained at the end of double inflation. Since the strong conversion between adiabatic and isocurvature perturbations occurs during the tachyonic instability region, the final spectrum of curvature perturbations is affected by the steep blue-tilted spectrum of isocurvature perturbations. Therefore the final $P_{\mathcal{R}}$ exhibits a steeper blue-tilted spectrum than predicted by Eq. (4.13).

This tells us that the correlation between adiabatic and isocurvature perturbations is important to correctly estimate the final spectra. The slow-roll results (4.13) and (4.14) typically show limitations when the correlation is strong. Note that in Fig. 14 all spectra $P_{\mathcal{R}}$, P_S, and P_C in the case (a) exhibit almost the same blue spectral indices due to the strong correlation.

Although the case (a) corresponds to the one with rather steep blue-tilted spectra, one can obtain nearly scale-invariant spectra by choosing small values of γ and δ relative to unity. For example, the case (b) in Fig. 14 corresponds to the one with $\gamma\simeq0.04\ll1$ and $\delta\simeq0.6(c^2-1)\lesssim0.2$ for $N_k\lesssim63$.

In this case both the adiabatic and isocurvature spectra generated for $\phi>\phi_c$ are slightly blue tilted, as predicted by Eqs. (4.13) and (4.14). The conversion of perturbations occurs after the symmetry breaking as well, but the spectral indices are mostly inherited by the end of double inflation because both $P_{\mathcal{R}}$ and P_S have similar small spectral indices

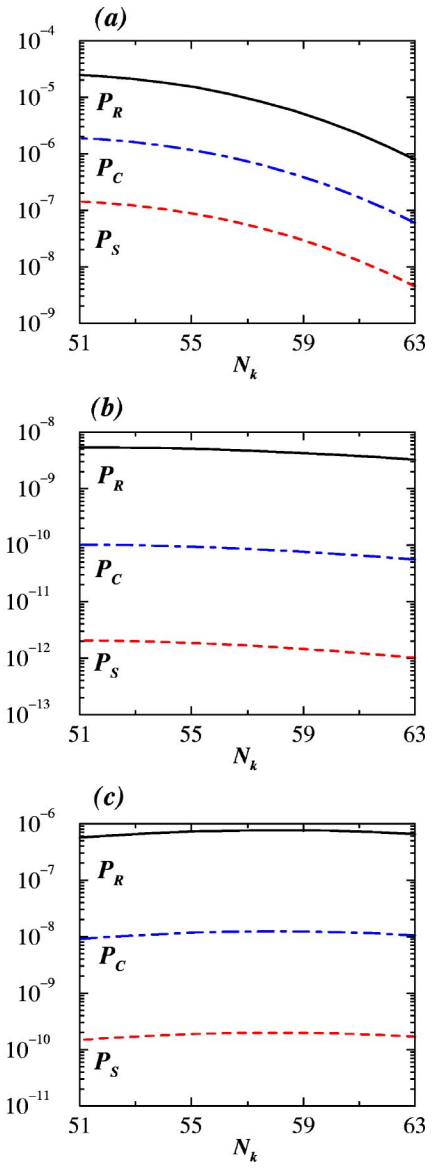

FIG. 14. The power spectra $P_{\mathcal{R}}$, P_S, and P_C for $g^2/\lambda=2$. Each case corresponds to (a) $M=7.0\times10^{-7}M_p$, $\lambda=1.0\times10^{-12}$, $m=2.0\times10^{-7}M_p$, $\phi_i=1.47\phi_c$, $\chi_i=1.0\times10^{-3}\chi_0$, (b) $M=8.5\times10^{-7}M_p$, $\lambda=9.0\times10^{-13}$, $m=2.0\times10^{-7}M_p$, $\phi_i=1.22\phi_c$, $\chi_i=5.0\times10^{-2}\chi_0$, and (c) $M=8.1\times10^{-7}M_p$, $\lambda=1.0\times10^{-12}$, $m=2.0\times10^{-7}M_p$, $\phi_i=1.11\chi_c$, $\chi_i=1.0\times10^{-3}\chi_0$.

at $\phi=\phi_c$. As shown in Fig. 14 all of $P_{\mathcal{R}}$, P_S, and P_C exhibit slightly blue-tilted spectra at the end of double inflation.

One may consider that the tachyonic growth of large-scale perturbations may lead to red-tilted spectra. In the cases (a) and (b) all modes shown in Fig. 14 (corresponding to $51\lesssim N_k\lesssim63$) are already left far outside the horizon when the field reaches $\phi=\phi_c$. Since the physical momenta satisfy $k/a\ll H$ for all these modes, the tachyonic growth rate of perturbations is practically the same for modes corresponding to $51\lesssim N_k\lesssim63$. Therefore in the cases (a) and (b) the presence of the tachyonic region does not yield red-tilted spectra.

However, if the duration in the first stage of inflation is short, it is possible to obtain the red-tilted spectrum on smaller scales. For example, in the case (c) illustrated in Fig. 14, the e-folds during the first stage of inflation are $N_1\sim7.5$ (the total e-folds are $N\sim65$). The modes corresponding to $N_k\gtrsim58$ crossed the horizon before the field reaches the point $\phi=\phi_c$. For these modes the spectra of perturbations are blue tilted as are the cases of (a) and (b).

In contrast, the smaller-scale modes with $N_k\lesssim58$ crossed the horizon after the symmetry breaking, in which case one has a red-tilted spectrum due to the negative χ mass (see Fig. 14). The case (c) corresponds to slightly red-tilted spectra with $|\delta|\ll1$. If the values of $|\delta|$ are increased, we have steeper negative tilts than shown in Fig. 14. It is very interesting that such a variety of spectra can be obtained by different choices of model parameters and initial conditions.

In Fig. 13 we find that the absolute values of the mass $\mu_s^2/(3H^2)$ and $\dot{\theta}/H$ change during double inflation, while the variation of $\mu_Q^2/(3H^2)$ is small. In addition, although the mass $\mu_s^2/(3H^2)$ is positive initially, it changes sign after the symmetry breaking. Therefore, to use the ''frozen'' positive mass in Eq. (2.20) is not typically valid, thereby leading to errors in the final consistency relations. And while the correlation is suppressed for $\phi>\phi_c$, the tachyonic growth of the fluctuation $\delta\chi$ yields strong correlation after the symmetry breaking.

Numerically we found that the correlation ratio r_C is very close to unity at the end of double inflation (see Fig. 14). This is associated with the enhancement of $\mathcal{R}$ and Φ shown in Fig. 12. In Fig. 15 the first consistency relation shows good agreement with the numerical results in the cases (a) and (c), while the case (b) is not so good. In the cases (a) and (c) we chose the initial value $\chi_i=10^{-3}\chi_0$, while the case (b) corresponds to $\chi_i=0.04\chi_0$. In the former cases one has $\dot{\theta}/H$ of order 0.001 around the scale $N_k\sim60$, but $\dot{\theta}/H$ is larger by more than one order of magnitude in the latter case. The correlation is negligible at horizon crossing in the cases (a) and (c), but in case (b) it is not. This is the main reason for the deviation from the first consistency relation in the case (b). In fact, we have numerically checked that the first consistency relation tends to agree with the numerical results as we decrease the initial χ (i.e., smaller $\dot{\theta}/H$). Note that r_C grows close to unity during the second stage of inflation, whose behavior is almost independent of the value of r_C at horizon crossing.

Our numerical simulations show that the second consistency relation does not agree with the one obtained by the definition (2.37) (see Fig. 15). In particular, although r_T is positive definite in Eq. (2.37), negative values of r_T appear when we use Eq. (2.42), implying strong deviations from the second consistency relation (note that in Fig. 15 we showed the absolute values of r_T). Again, this is mainly due to the violation of the assumption of the constant masses and $\dot{\theta}/H$ during the tachyonic instability region.

Notice also that if we use the slow-roll expression for x in Eq. (2.39) this does not provide the correct value of the correlation r_C. In the case (a) of Fig. 15, for example, we have

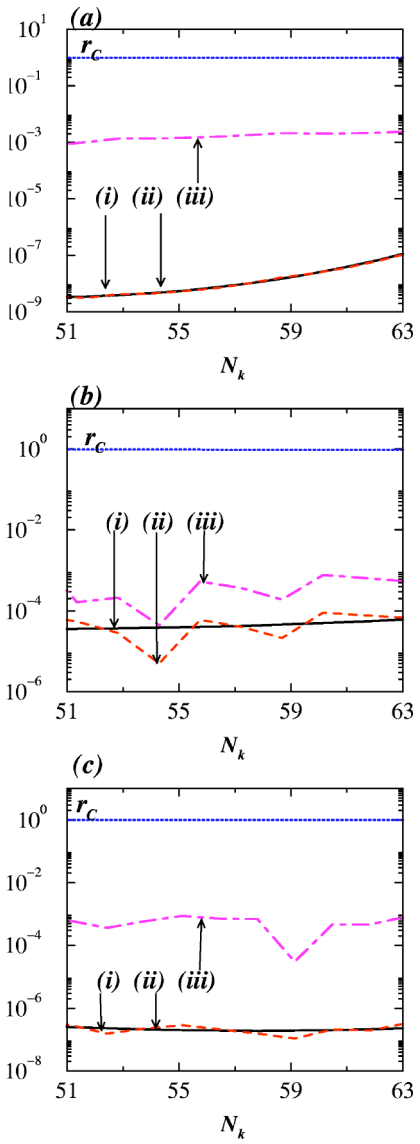

FIG. 15. The correlation r_C and the ratio r_T that are derived by using Eq. (2.36) and the two consistency relations (2.41) and (2.42), which are denoted by (i), (ii), and (iii), respectively. We show the cases (i), (ii), and (iii) by solid curves, dashed curves, and dot-dashed curves, respectively. Note that in the case (2.42) we have taken the absolute value of r_T. The initial conditions for the three cases are the same as in Fig. 14.

$(\dot{\theta}/H)_k \sim 0.001$ and $\zeta_k \sim 0.37$ around $N_k = 60$. Therefore Eq. (2.39) leads to $x \sim 0.005$ and $r_C \sim 0.005 \ll 1$. This is significantly different from the numerical value of r_C close to unity. We have to integrate the $\dot{\theta}/H$ term from the horizon crossing to the end of inflation in order to correctly estimate the final value of r_C. Note that when we evaluate x in Eq. (2.38) numerically the first consistency relation shows excellent agreement with the numerical results [as in the cases (a) and (c) in Fig. 15], as long as the correlation is not large at horizon crossing.

When the χ mass is light ($|\delta| \lesssim 1$) and the second phase of inflation takes place, we find that the correlation r_C is close to 1, even changing the values of g^2/λ to be of order unity. The correlation is also expected to be strong in other models of double inflation with a tachyonic instability.

V. CONCLUSIONS

In this paper we studied the correlation of adiabatic and isocurvature perturbations generated in inflationary scenarios with two phases of inflation (double inflation). We made a detailed multiparameter numerical analysis of the power spectra relevant for the cosmic microwave background and large-scale structure. We also studied the validity of the inflationary consistency relations derived from slow-roll analysis for two different models of double inflation—the two noninteracting/interacting massive scalar fields and the supersymmetric model with a tachyonic (spinodal) instability separating the two phases of inflation.

In single-field inflationary scenarios, the slow-roll approximation is typically reliable except near the end of inflation. In the case of multiple scalar fields, however, we need to be more careful in the use of the slow-roll approximation. If one of the scalar field is quickly suppressed and another scalar field leads to inflation with more than 60 *e*-folds, perturbations relevant for large-scale structure are effectively described by the single-field inflationary scenario. However, when both scalar fields are of the same order around 60 *e*-folds before the end of double inflation, we are faced with limitations in the use of slow-roll results. In this case the slow-roll parameter of the heavy scalar field is already large around the end of the first stage of inflation.

The assumption of the slow variation of the effective masses of ''adiabatic'' and ''entropy'' fields, which is used to obtain the spectra of perturbations analytically, is often not valid in the context of the double-inflationary scenarios. This is reflected in our results where we found that the slow-roll derived correlation r_C and three spectral indices $n_{\mathcal{R}}$, n_S, and n_C do not agree well with the full numerical simulations, especially when the correlation is strong. If the correlation is negligibly small *at horizon crossing*, the first consistency relation (2.41) shows good agreement with our numerical results [see the cases (a) and (b) in Fig. 4 and the cases (a) and (c) in Fig. 15]. This is consistent with the result of Wands *et al.* that the first consistency relation was obtained only by assuming a vanishingly small correlation at horizon crossing [34]. In the case where slow-roll conditions are violated at horizon crossing, which can occur in double-inflationary scenarios, we find that numerical results exhibit some deviation from the first consistency relation (2.41) [see the case (c) in Fig. 4 and the case (b) in Fig. 15].

The second consistency relation (2.42) is more strongly affected by the change of the entropy/adiabatic mass and the scalar field velocity angle $\dot{\theta}$ during double inflation, thereby showing stronger deviations especially when the correlation is large. These results suggest the necessity of numerical analysis—or a refined analytical treatment—in order to correctly estimate the final power spectra, spectral indices, and correlations of perturbations.

We also found that a wide variety of power spectra and correlations can be obtained, depending on the parameters of the models considered. In the case of noninteracting massive

scalar fields, two important quantities determine the strength of the correlation: the ratio of the two scalar fields ($\tan\alpha_*$) and the ratio of the two masses (R). We made a complete classification for several different cases to understand the correlation appropriately.

When the interaction between two scalar fields ($g^2\phi^2\chi^2$) is introduced, this can lead to a blue spectrum of isocurvature perturbations if the mass of the entropy field perturbation is larger than the Hubble rate. However, the heavy field χ is soon suppressed toward the potential valley at $\chi=0$, in which case the correlation between adiabatic and isocurvature perturbations is weak.

Therefore the spectrum of the adiabatic perturbation is typically slightly red tilted as in the case with $g=0$. In this model we also found an interesting parameter range where large values of g and χ lead to rather steeply red-tilted spectra of strong correlated adiabatic and isocurvature perturbations toward large scales. This comes from the negative mass of the entropy field perturbation with comparable values of two scalar fields.

In the double-inflationary scenario motivated by supersymmetric theories, the correlation is found to be very large ($r_C \simeq 1$). This is associated with a tachyonic growth of the entropy field perturbation during the second stage of double inflation. This strong correlation also yields a mixture of adiabatic and isocurvature perturbations after the symmetry breaking, thereby modifying the spectra of perturbations generated during the first stage of inflation. We found that a variety of power spectra can be obtained by making use of this conversion mechanism.

In the original version of the hybrid inflation with potential (4.1) [43], the field χ is strongly suppressed because of its large effective mass before the symmetry breaking. Inflation ends by a rapid rolling of the field χ after the symmetry breaking at $\phi=\phi_c$. Since the field χ has essentially no homogeneous component at $\phi=\phi_c$, the decomposition of χ between the homogeneous field $\chi(t)$ and the perturbative part $\delta\chi(\mathbf{x},t)$ is not necessarily valid. When χ is negligibly small at $\phi=\phi_c$, we need to go beyond the perturbation theory using the spatial distribution of the field $\chi(\mathbf{x},t)$ as in Ref. [59].

Note, however, that in the case of double inflation the field χ is hardly suppressed for $\phi>\phi_c$ due to the light χ mass ($|\delta| \lesssim 1$). Then we are free from the problem of the decomposition of χ, in which case our linear analysis can be reliable. We also made some simulations including the backreaction effect of field fluctuations as the Hartree approximation and obtained similar results as found in this work.

In our work we analyzed two models of double inflation given by the potentials (3.1) and (4.1). Since these potentials include most of the basic properties of the double inflation, it should be fairly easy to extend our analysis to other double-inflation models motivated by particle physics.[10]

[10]In some models of two-field inflation considered as in Refs. [15,28,32], the second stage of inflation is absent. In this case the first consistency relation (2.41) is expected to be valid, while the second one (2.42) may be model dependent [34].

It is really encouraging that double-inflation models lead to strong correlations over wide ranges of their parameter spaces. This suggests that searches for correlations in the CMB may yield interesting information and constraints on such models and motivates the development of enhanced slow-roll approximations which can accurately predict the full numerical results.

ACKNOWLEDGMENTS

We thank Nicola Bartolo, Christopher Gordon, Julien Lesgourgues, Alexei Starobinsky, Jun'ichi Yokoyama, and particularly Carlo Ungarelli and David Wands, for useful discussions. S.T. is also thankful for financial support from the JSPS (No. 04942). The research of B.B. is supported under PPARC grant PPA/G/S/2000/00115. D.P. is thankful for financial support from the Monbukagakusho Young Foreign Researcher summer program and grateful to RESCEU for hospitality. S.T. is grateful to Stanislav Alexeyev and Alexey Toporensky for kind hospitality during his stay at the Sternberg Astronomical Institute, Moscow State University.

APPENDIX: NUMERICAL METHODS TO EVALUATE POWER SPECTRA AND CORRELATIONS

Let us explain the general numerical method used to calculate power spectra and correlations in the context of multifield inflation. We treat Q_σ and δs as independent stochastic variables for the modes deep inside the Hubble radius. Then we have to do two numerical runs in order to evaluate $P_{\mathcal{R}}$, P_S, and P_C. One run corresponds to the Bunch-Davies vacuum state for Q_σ and $\delta s=0$ for the entropy field perturbation, in which case we get the solutions $\mathcal{R}=\mathcal{R}_1$ and $S=S_1$. Another corresponds to the Bunch-Davies vacuum state for δs and $Q_\sigma=0$ for the adiabatic field perturbation, in which case we have $\mathcal{R}=\mathcal{R}_2$ and $S=S_2$.

Then each power spectrum can be expressed in terms of $\mathcal{R}_1$, $\mathcal{R}_2$, S_1, and S_2, as

$$P_{\mathcal{R}}=\frac{k^3}{2\pi^2}(|\mathcal{R}_1|^2+|\mathcal{R}_2|^2), \tag{A1}$$

$$P_S=\frac{k^3}{2\pi^2}(|S_1|^2+|S_2|^2), \tag{A2}$$

$$P_C=\frac{k^3}{2\pi^2}|\mathcal{R}_1S_1+\mathcal{R}_2S_2|. \tag{A3}$$

From this it is easy to show that the correlation $r_C=P_C/\sqrt{P_{\mathcal{R}}P_S}$ is in the range $r_C \leqslant 1$.

If we run the numerical code only once by using the initial conditions where both Q_σ and δ_s are in the vacuum state, we then get $\mathcal{R}=\mathcal{R}_1+\mathcal{R}_2$. In this case the power spectrum of $\mathcal{R}$ yields $P_{\mathcal{R}}=(k^3/2\pi^2)|\mathcal{R}_1+\mathcal{R}_2|^2$, which is different from Eq. (A1). As long as the perturbations are stochastic random variables initially, it is required to adopt the method described in Eqs. (A1)–(A3).

[1] J. M. Bardeen, Phys. Rev. D **22**, 1882 (1980); S. Mollerach, Phys. Lett. B **242**, 158 (1990); Phys. Rev. D **42**, 313 (1990); H. Kodama and M. Sasaki, Int. J. Mod. Phys. A **1**, 265 (1986); **2**, 491 (1987); D. Salopek, Phys. Rev. D **45**, 1139 (1992).

[2] V. N. Lukash, Sov. Phys. JETP **52**, 807 (1980); V. F. Mukhanov and G. V. Chibisov, JETP Lett. **33**, 532 (1981); S. W. Hawking, Phys. Lett. **115B**, 295 (1982); A. A. Starobinsky, *ibid.* **117B**, 175 (1982); A. H. Guth and S. Y. Pi, Phys. Rev. Lett. **49**, 1110 (1982); J. M. Bardeen, P. J. Steinhardt, and M. S. Turner, Phys. Rev. D **28**, 679 (1983); D. H. Lyth, *ibid.* **31**, 1792 (1985).

[3] D. H. Lyth and A. Riotto, Phys. Rep. **314**, 1 (1999).

[4] J. A. Adams, G. G. Ross, and S. Sarkar, Nucl. Phys. **B503**, 405 (1997); J. Lesgourgues, *ibid.* **B582**, 593 (2000).

[5] A. D. Linde, Phys. Lett. **158B**, 375 (1985); A. A. Starobinsky, JETP Lett. **42**, 152 (1985); L. A. Kofman, Phys. Lett. B **173**, 400 (1986); A. D. Linde and Kofman, Nucl. Phys. **B282**, 555 (1987); Salopek [1].

[6] H. Kodama and M. Sasaki, Prog. Theor. Phys. Suppl. **78**, 1 (1984).

[7] V. F. Mukhanov, H. A. Feldman, and R. H. Brandenberger, Phys. Rep. **215**, 293 (1992).

[8] C. Gordon, D. Wands, B. A. Bassett, and R. Maartens, Phys. Rev. D **63**, 023506 (2001).

[9] J. c. Hwang and H. Noh, Class. Quantum Grav. **19**, 527 (2002).

[10] L. Amendola, C. Gordon, D. Wands, and M. Sasaki, Phys. Rev. Lett. **88**, 211302 (2002).

[11] J. c. Hwang, Astrophys. J. **375**, 443 (1991).

[12] W.-L. Lee and L.-Z. Fang, Europhys. Lett. **56**, 904 (2001).

[13] D. Polarski and A. A. Starobinsky, Nucl. Phys. **B385**, 623 (1992).

[14] D. Polarski and A. A. Starobinsky, Phys. Rev. D **50**, 6123 (1994).

[15] A. A. Starobinsky and J. Yokoyama, gr-qc/9502002.

[16] J. Garcia-Bellido and D. Wands, Phys. Rev. D **52**, 6739 (1995); **53**, 5437 (1996).

[17] M. Sasaki and E. D. Stewart, Prog. Theor. Phys. **95**, 71 (1996).

[18] A. D. Linde and V. Mukhanov, Phys. Rev. D **56**, 535 (1997).

[19] T. Chiba, N. Sugiyama, and J. Yokoyama, Nucl. Phys. **B530**, 304 (1998).

[20] V. F. Mukhanov and P. J. Steinhardt, Phys. Lett. B **422**, 52 (1998).

[21] J. Lesgourgues and D. Polarski, Phys. Rev. D **56**, 6425 (1997).

[22] M. Sasaki and T. Tanaka, Prog. Theor. Phys. **99**, 763 (1998).

[23] Y. Nambu and A. Taruya, Class. Quantum Grav. **15**, 2761 (1998).

[24] D. Langlois, Phys. Rev. D **59**, 123512 (1999).

[25] T. Kanazawa, M. Kawasaki, N. Sugiyama, and T. Yanagida, Phys. Rev. D **61**, 023517 (2000).

[26] D. Langlois and A. Riazuelo, Phys. Rev. D **62**, 043504 (2000).

[27] D. Wands, K. A. Malik, D. H. Lyth, and A. R. Liddle, Phys. Rev. D **62**, 043527 (2000).

[28] S. Tsujikawa and H. Yajima, Phys. Rev. D **62**, 123512 (2000).

[29] J. c. Hwang and H. Noh, Phys. Lett. B **495**, 277 (2000).

[30] N. Bartolo, S. Matarrese, and A. Riotto, Phys. Rev. D **64**, 083514 (2001).

[31] N. Bartolo, S. Matarrese, and A. Riotto, Phys. Rev. D **64**, 123504 (2001).

[32] A. A. Starobinsky, S. Tsujikawa, and J. Yokoyama, Nucl. Phys. **B610**, 383 (2001).

[33] S. Groot Nibbelink and B. J. van Tent, Class. Quantum Grav. **19**, 613 (2002).

[34] D. Wands, N. Bartolo, S. Matarrese, and A. Riotto, Phys. Rev. D **66**, 043520 (2002).

[35] D. H. Lyth and D. Wands, Phys. Lett. B **524**, 5 (2002); K. Enqvist and M. S. Sloth, Nucl. Phys. **B626**, 395 (2002); T. Moroi and T. Takahashi, Phys. Lett. B **522**, 215 (2001); **539**, 303(R) (2002); N. Bartolo and A. R. Liddle, Phys. Rev. D **65**, 121301 (2002); T. Moroi and T. Takahashi, *ibid.* **66**, 063501 (2002); D. H. Lyth, C. Ungarelli, and D. Wands, *ibid.* **67**, 023503 (2003); M. S. Sloth, hep-ph/0208241.

[36] A. Taruya and Y. Nambu, Phys. Lett. B **428**, 37 (1998); B. A. Bassett, D. I. Kaiser, and R. Maartens, **455**, 84 (1999); F. Finelli and R. H. Brandenberger, Phys. Rev. Lett. **82**, 1362 (1999); B. A. Bassett and F. Viniegra, Phys. Rev. D **62**, 043507 (2000); F. Finelli and R. H. Brandenberger, *ibid.* **62**, 083502 (2000); B. A. Bassett, M. Peloso, L. Sorbo, and S. Tsujikawa, Nucl. Phys. **B622**, 393 (2002); S. Tsujikawa and B. A. Bassett, Phys. Lett. B **536**, 9 (2002).

[37] R. Trotta, A. Riazuelo, and R. Durrer, Phys. Rev. Lett. **87**, 231301 (2001).

[38] M. Bucher, K. Moodley, and N. Turok, Phys. Rev. D **62**, 083508 (2000).

[39] N. Bartolo, S. Matarrese, and A. Riotto, Phys. Rev. D **65**, 103505 (2002); F. Bernardeau and J. P. Uzan, *ibid.* **66**, 103506 (2002); astro-ph/0209330.

[40] F. Finelli and R. Brandenberger, Phys. Rev. D **65**, 103522 (2002).

[41] J. Martin and D. J. Schwarz, Phys. Rev. D **62**, 103520 (2000).

[42] S. M. Leach, A. R. Liddle, J. Martin, and D. J. Schwarz, Phys. Rev. D **66**, 023515 (2002).

[43] A. D. Linde, Phys. Rev. D **49**, 748 (1994).

[44] E. J. Copeland, A. R. Liddle, D. H. Lyth, E. D. Stewart, and D. Wands, Phys. Rev. D **49**, 6410 (1994).

[45] L. Randall, M. Soljacic, and A. H. Guth, Nucl. Phys. **B472**, 377 (1996).

[46] G. R. Dvali, Q. Shafi, and R. Schaefer, Phys. Rev. Lett. **73**, 1886 (1994).

[47] G. G. Ross and S. Sarkar, Nucl. Phys. **B461**, 597 (1996); J. A. Adams, G. G. Ross, and S. Sarkar, Phys. Lett. B **391**, 271 (1997).

[48] R. Jeannerot, Phys. Rev. D **56**, 6205 (1997).

[49] E. Halyo, Phys. Lett. B **387**, 43 (1996); P. Binetruy and G. R. Dvali, *ibid.* **388**, 241 (1996).

[50] C. Panagiotakopoulos, Phys. Rev. D **55**, 7335 (1997).

[51] A. D. Linde and A. Riotto, Phys. Rev. D **56**, 1841 (1997).

[52] B. A. Bassett, F. Tamburini, D. I. Kaiser, and R. Maartens, Nucl. Phys. **B561**, 188 (1999).

[53] M. Sasaki, Prog. Theor. Phys. **76**, 1036 (1986); V. F. Mukhanov, Sov. Phys. JETP **68**, 1297 (1988).

[54] A. A. Starobinsky, Pisma Zh. Eksp. Teor. Fiz. **55**, 477 (1992) [JETP Lett. **55**, 489 (1992)].

[55] S. M. Leach, M. Sasaki, D. Wands, and A. R. Liddle, Phys. Rev. D **64**, 023512 (2001).

[56] D. Boyanovsky, D. Cormier, H. J. de Vega, R. Holman, and S. P. Kumar, Phys. Rev. D **57**, 2166 (1998).

[57] D. Cormier and R. Holman, Phys. Rev. D **60**, 041301 (1999); **62**, 023520 (2000).
[58] S. Tsujikawa and T. Torii, Phys. Rev. D **62**, 043505 (2000); S. Tsujikawa, *ibid.* **61**, 083516 (2000).
[59] G. N. Felder, J. Garcia-Bellido, P. B. Greene, L. Kofman, A. D. Linde, and I. Tkachev, Phys. Rev. Lett. **87**, 011601 (2001); G. N. Felder, L. Kofman, and A. D. Linde, Phys. Rev. D **64**, 123517 (2001).
[60] M. Bastero-Gil, S. F. King, and J. Sanderson, Phys. Rev. D **60**, 103517 (1999).
[61] R. Easther and K. i. Maeda, Class. Quantum Grav. **16**, 1637 (1999).
[62] J. Garcia-Bellido and A. D. Linde, Phys. Rev. D **57**, 6075 (1998).